# Light-directed evolution of dynamic, multi-state, and computational protein functionalities

Vojislav Gligorovski[1], Marco Labagnara[1], Sahand Jamal Rahi[1,*]

[1]: Laboratory of the Physics of Biological Systems, Institute of Physics, EPFL, Switzerland

[*]: sahand.rahi@epfl.ch

## Abstract

Directed evolution is a powerful method in biological engineering. Current approaches were devised for evolving steady-state properties such as enzymatic activity or fluorescence intensity. A fundamental problem remains how to evolve dynamic, multi-state, or computational functionalities, e.g., folding times, on-off kinetics, state-specific activity, stimulus-responsiveness, or switching and logic capabilities. These require applying selection pressure on all of the states of a protein of interest (POI) and the transitions between them. We realized that optogenetics and cell cycle oscillations could be leveraged for a novel directed evolution paradigm ('optovolution') that is germane for this need: We designed a signaling cascade in budding yeast where optogenetic input switches the POI between off (0) and on (1) states. In turn, the POI controls a Cdk1 cyclin, which in the re-engineered cell cycle system is essential for one cell cycle stage but poisonous for another. Thus, the cyclin must oscillate (1-0-1-0…) for cell proliferation. In this system, evolution can act efficiently on the dynamics, transient states, and input-output relations of the POI in every cell cycle. Further, controlling the pacemaker, light, directs and tunes selection pressures. Optovolution is *in vivo*, continuous, self-selecting, and genetically robust. We first evolved two optogenetic systems, which relay 0/1 input to 0/1 output: We obtained 25 new variants of the widely used LOV transcription factor El222. These mutants were stronger, less leaky, or green- and red-responsive. The latter was conjectured to be impossible for LOV domains but is needed for multiplexing and lowering phototoxicity. Evolving the PhyB-Pif3 optogenetic system, we discovered that loss of *YOR1* makes supplementing the expensive and unstable chromophore phycocyanobilin (PCB) unnecessary. Finally, we demonstrate the generality of the method by creating and evolving a destabilized rtTA transcription factor, which performs an AND operation between transcriptional and doxycycline input. Optovolution makes coveted, difficult-to-change protein functionalities evolvable.

# Introduction

Directed evolution has been critical to improving and diversifying many of the molecular tools currently used in research and industry such as enzymes[1–5], fluorescent proteins[6,7], and antibodies[8,9]. The method relies on mutations, either from standing variation or mutagenesis, to diversify genetically encoded molecules. These are then screened for a desired function. The mutation-screen cycle is generally repeated to bring the molecules' functionalities closer to the desired goal.[10]

One important innovation in the field has been to couple a molecule of interest's functionality to organismal proliferation and fitness, so that continuous *in vivo* self-selection obviates labor-intensive screening[1,11–14]. Another important advance has been to elevate mutation rates only for to-be-evolved genes[15–17].

Despite major progress, current continuous directed evolution methods remain inherently only suited for steady-state functionalities such as enzymatic activity or fluorescence intensity. This is because existing approaches only screen and select for one property of a POI at a time. However, many natural and synthetic biological molecules involve more than one state. In fact, all signal transduction, control, and computation necessarily involve changes between states, usually, on (1) or off (0). For example, many transcription factors and kinases are controlled by upstream signals. Beyond information relays, proteins and circuits often integrate multiple inputs for cellular decisions, e.g., the amount of DNA damage and arrest times jointly determine the DNA damage checkpoint override decision.[18] Such computational capabilities are highly desirable in engineering. Building more intelligent cells needs logic gating of inputs, which is generally designed rationally.[19–23] Evolving proteins with such functionalities requires, in principle, that selection pressure is simultaneously applied on all of the computations, that is, all input-output relationships of the POI. Otherwise, if directed evolution is performed for only one state, e.g., the enzymatic activity in the on (1) state, the other states or the ability to switch to them can be corrupted.[24] For example, long-term directed evolution of GPCRs under constant ligand concentrations reduces ligand responsiveness.[25]

To cope with this limitation, researchers resort to alternating directed evolution campaigns for each of the different states of the POI at a time[26–37]. For example, a bioengineer will assay for on (1) activity under inducing conditions, select candidate mutants, then assay for off (0) activity under non-inducing conditions, select mutants, and repeat this process. Such sequences of alternating directed evolution experiments are not only laborious but do not necessarily succeed, as we show for the –uracil/+5-fluoroorotic acid (-Ura/+FOA) selection/counterselection method[38]. The fundamental weakness of this work-around to evolving multi-state POIs is that in many cases, it is highly probable for mutations to corrupt the states that are not under selection pressure. For example, to decrease leakiness in the (0)

63 off state, it is more likely to simply acquire loss-of-function mutations than to maintain (1) on state
64 activity. Furthermore, the kinetics of switching is very difficult to address with such approaches.

65 In summary, there is an unmet, broad need for better directed evolution approaches for dynamic,
66 multi-state, and computational protein functionalities. Here, we present the first paradigm that is
67 germane for these goals, which we name 'optovolution'. In contrast to previous approaches,
68 optovolution was designed with a mechanism to evolve all input-output relationships of a POI as well
69 as switches among them during the same campaign. Two conceptual advances, explained in more
70 detail below, underlie optovolution: By engineering a POI to control a cell cycle regulator that is
71 essential for one step of cell proliferation but toxic to another, the POI must evolve or maintain the
72 ability to switch between 0 and 1 outputs rapidly. In turn, by controlling the input to the POI with light
73 and optogenetics, this selection pressure is shaped by an external signal that is dynamic at the
74 timescale of a cell cycle and that temporally segregates the effects of the 0 and 1 states of the POI.

75 We apply optovolution to three systems, the optogenetic transcriptional system El222 and the
76 optogenetic dimerization switch PhyB-Pif3, which relay light input by switching on (1) or off (0), and
77 an AND gate, in which a degron-tagged rtTA transcription factor is controlled by transcription and
78 doxycycline:

79 1) LOV domains make up the core of most non-ion-channel optogenetic systems[39–53], presumably
80 because they are small, reliable, and do not need exogenous chromophores. Interest in LOV domains
81 is reflected in multiple diversification campaigns[34,54–56]. The LOV transcription factor El222, in
82 particular, is widely used in many biological models from cell-free systems[57], to bacteria[58], yeast[59,60],
83 mammalian cell lines[61,62], and zebrafish[63]. (See **Supplementary Note 1** for additional information
84 regarding El222.) However, less leaky or more light-sensitive variants are needed. A comparison of
85 different inducible transcriptional systems showed that El222 controlling the standard *light-inducible*
86 *promoter* (*LIP*) has both more off-state leakiness and lower on-state strength than, for example, the
87 *GAL1* promoter, demonstrating the need for improvements.[55] For example, for light-controlled
88 expression of toxic genes, leakiness creates selection pressure for loss-of-function mutations. On the
89 other hand, maximal transcriptional output with wild-type El222 is associated with phototoxicity.
90 Further, all existing LOV systems are only activated by blue light, which has several drawbacks: First,
91 blue light of sufficient intensity causes phototoxicity.[55,64] Secondly, blue light penetrates skin poorly.[65]
92 Thirdly, the advantages of LOV domains cannot be leveraged to control different optogenetic systems
93 independently in an organism. Ideally, one could build optogenetic systems based on LOV domains,
94 change their color responsiveness by mutations, and thereby straightforwardly combine different
95 systems. Instead, for multiplexing, one currently has to engineer optogenetic systems using different
96 light-sensitive domains, each representing a challenging endeavor.[66–69] In fact, substantially changing
97 the color responsiveness of LOV domains was conjectured to be "likely impossible" based on the lack

98 of such known natural or engineered examples and physicochemical considerations.[70] Previous work
99 to shift the excitation spectrum of LOV domains was based on rational design and achieved a maximal
100 shift of 8 nm in the absorption peak further toward UV *in vitro*.[71] Using optovolution, we evolved 25
101 new variants of El222, including more light sensitive, less leaky, or green- and red-responsive mutants,
102 paving the way for new applications. In traditional directed evolution approaches, multiple paths to
103 by-pass our desired goals would have existed involving constitutively on or off mutants.

104 2) In the widely used PhyB-Pif3 system, PhyB and Pif3 dimerize in response to red light and
105 dissociate with far red light. The system is often used to change the intracellular localization of
106 proteins by fusing them to PhyB or Pif3 and anchoring the other dimerization partner to a specific
107 intracellular compartment[72,73]. For transcriptional induction, PhyB and Pif3 are fused to the Gal4
108 transcriptional activation domain (AD) and the Gal4 DNA binding domain (DBD), respectively.[74–76] For
109 use in yeast, *Caenorhabditis elegans*, and mammalian cells, the chromophore PCB has to be
110 supplemented.[72,74,77] The co-factor is expensive as well as light- and temperature-sensitive,
111 complicating experiments. In previous work, a biochemical pathway to convert heme to PCB was
112 introduced in different organisms.[77–80] This involved substantial genetic manipulation of the host
113 genome: Several transgenes had to be introduced, some of which needed to be targeted to
114 mitochondria, their expression levels needed to be optimized, and, in certain cases, endogenous
115 genes needed to be deleted. It is unclear whether there are already metabolic pathways in cells that
116 could be unlocked for PhyB-Pif3 to work more straightforwardly. Using optovolution, we found that
117 loss of function of *YOR1* makes PCB unnecessary in budding yeast. The use of *yor1Δ* substantially
118 simplifies applications and further directed evolution experiments. In traditional directed evolution
119 approaches, by-pass of our desired goal would have consisted of turning PhyB-Pif3 or its downstream
120 elements on constitutively in the absence of PCB.

121 3) While optovolution leverages light for control of directed evolution, the method is not specific
122 to engineering optogenetic systems. We demonstrate the general applicability of optovolution for
123 evolving dynamic, multi-state, and computational functionalities by evolving a non-optogenetic logic
124 gate POI. It is often desirable to condition the activity of molecules on two inputs. This requires an
125 AND logic gate, which is relatively difficult to create in biological systems compared to OR gates. For
126 example, researchers may wish to label a subset of cells for lineage tracing which express a certain
127 gene only at a specific time. To construct such a system, we used the doxycyclin-controlled
128 transcription factor rtTA[81] and fused it to a PEST degron[82]. This double-lock control represents an AND
129 gate function between transcriptional and doxycycline input. Without the degron, rtTA protein is
130 stable and thus, after translation, only controlled by doxycycline; responsiveness to further
131 transcriptional input could only happen in proliferating cells at the relatively slow timescale of
132 dilution. However, the initial PEST-rtTA fusion protein produced very weak output. With optovolution,

133 we evolved two mutants that conferred substantial output from the *tetO* promoter while maintaining
134 minimal leakiness. Note that in traditional directed evolution approaches for increasing the activity of
135 a POI, the degron could simply be corrupted. In contrast, optovolution maintains the dynamic
136 properties POIs by design.

137 Optovolution is a novel directed evolution paradigm for hitherto difficult-to-modify dynamic, multi-
138 state, and computational functionalities. We have demonstrated its usefulness by uncovering
139 unexpected and useful mutations improving three different important molecular tools.

# 140 Results

## 141 Conceptual requirements for evolving dynamic, multi-state, and computational 142 properties

143 We started with a general theoretical analysis. We considered how to evolve a POI with one or more
144 inputs and two outputs, 0 or 1 (Fig. 1 A). As in electrical engineering, 0 and 1 are useful abstractions,
145 which here represent molecular activity. Characterizing a POI in terms of input-output relationships
146 simplifies the description of a wide range of directed evolution goals. These may include increasing,
147 lowering, or changing the nature of the activity of outputs for specific inputs, or modifying the kinetics
148 of switching between outputs. 0 or 1 need not refer to absolute zero or the maximally attainable
149 activity (**Discussion**).

150 We considered that there can be a single input *i* to the POI, for example, transcriptional induction of
151 the POI, or a complex input $\boldsymbol{i}=(i_1,\ldots,i_n)$ such as specific phosphorylation patterns at *n* residues of the
152 POI. If each input channel is binary, there are $2^n$ input-output relations. In practice, the inputs will
153 ideally be controlled with optogenetics because administrating light, even for weeks, is precise,
154 dosable, cheap, and straightforward. Light input to the POI can in principle be direct or through
155 multiple intermediate steps. The POI itself does not have to be light sensitive. Optogenetic
156 transcription factors, kinases, and degrons can mediate the input to a POI. Although light control was
157 involved in a single screening step in past work[30], the general power of optogenetics for directing
158 evolution has hitherto not been recognized (**Discussion**). As output, the POI may, for example,
159 transcriptionally activate, phosphorylate, or degrade its targets, for example.

160 One could in principle use the same system with chemical inputs to the POI instead of light input.
161 However, the need for repeatedly changing the cell culture medium makes directed evolution with
162 optogenetic control of the inputs to the POI much preferable, if feasible. This is why we refer to our
163 method as 'optovolution'.

164

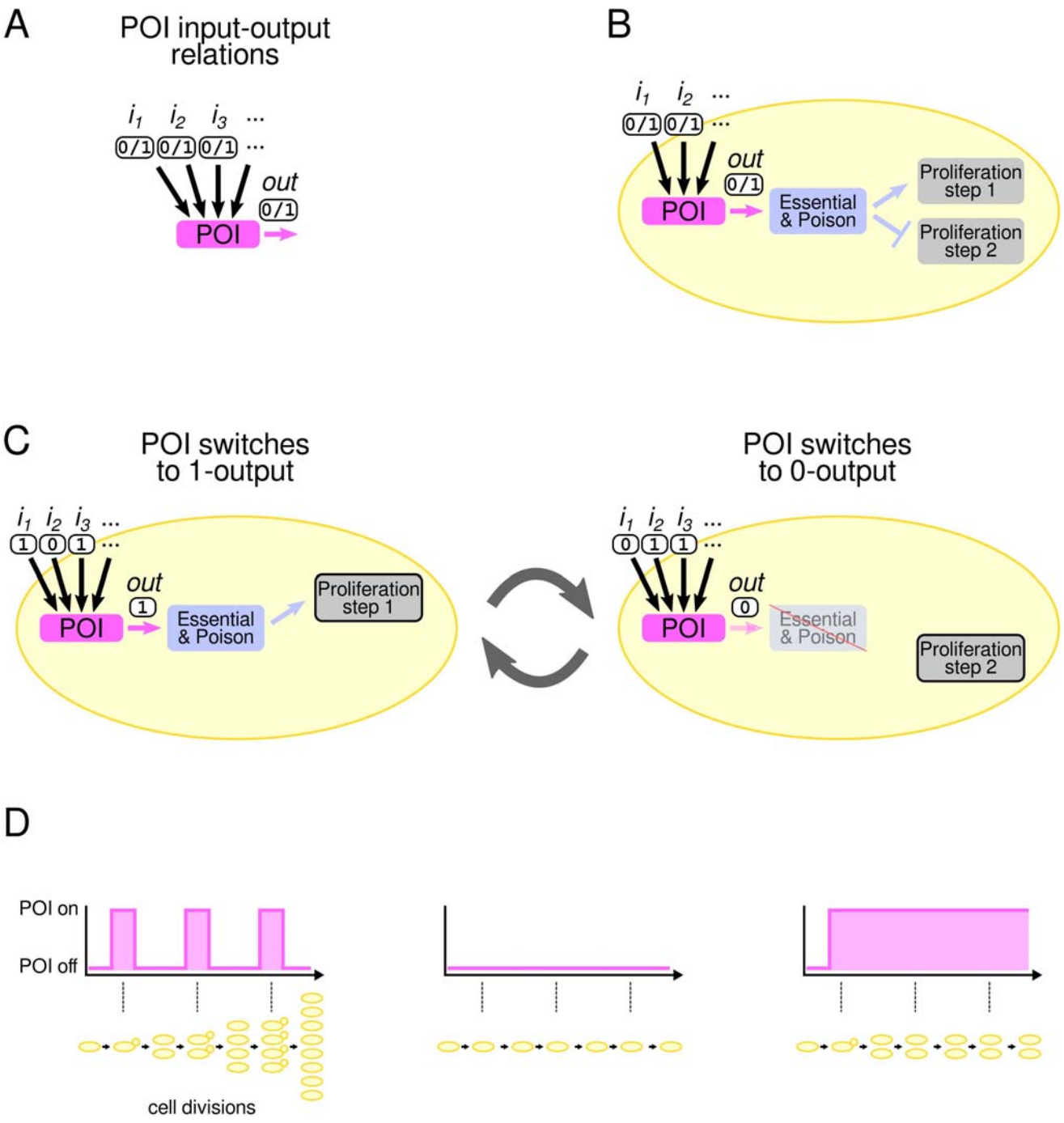


Figure 1. Conceptualization of optovolution. A: The POI has one or multiple inputs and one output. Inputs and output are idealized as having two states, on (1) or off (0). B. In optovolution, the POI controls a cellular regulator that is essential for one step in cellular proliferation but poisonous for another. The inputs to the POI are most conveniently controlled by light, mediated by optogenetic systems, which are not shown. C. By cycling the inputs to the POI, the POI switches output states and drives cycles of cellular proliferation. D. Cells only proliferate with repeated 1-0-1-0-… output pulses of the POI, not continuously on (1) or off (0) output, in a mutationally robust manner.

173 For such a broad set of possible inputs and outputs, the main conceptual challenge was to find a
174 mechanism to perform selection on each input-output relationship of the POI and the kinetics of the
175 transitions. We suppose that the inputs are labeled $i_a$, $i_b$, $i_c$, $i_d$, … and correspond to desired POI
176 outputs 1, 0, 1, 0, … We realized that we could perform directed evolution on this system if we made
177 the POI fully control a cellular regulator that was essential for one step in cell proliferation but
178 poisonous for another (Fig. 1 B, C). In such a system, if the POI switches between 1-0-1-0-… outputs,
179 driven by repeated cycles of inputs $i_a$-$i_b$-$i_c$-$i_d$-…, then cells will proliferate maximally (Fig. 1 D). Any
180 error, either in switching speed or state, e.g., POI output sequence 1-1-1-0-…, will cause skipped cell
181 cycles. This incurs a large fitness penalty, which gives an advantage to mutants with better fidelity to
182 the desired input-output relationships. There is freedom in devising protocols for the $i_a$-$i_b$-$i_c$-$i_d$-…
183 inputs. How to sequence the inputs optimally represents an interesting mathematical problem, which
184 we solve for time-independent protocols in **Supplementary Mathematical Analysis**.

185 Tunability of the selection pressure is of high practical importance for directed evolution. In our
186 conceptualized system, the strength and timing of the inputs to the POI would be controlled by light.
187 Therefore, the selection pressure on each state and on the kinetics of the transitions would be
188 straightforwardly tunable. For example, input-output relationships could be challenged by
189 administering light input that is too weak or too strong and then directed evolution would be
190 expected to improve the input-output by mutational adaptations. Similarly, engaging and releasing
191 the POI early or, alternatively, with delays, would force adaptations toward improved POI kinetics.
192 Also, differently engineered genetic backgrounds and different growth conditions would allow further
193 control over selection pressures on POI states and transitions (**Discussion**). Decades of research into
194 control of growth, metabolism, and the cell cycle could be used for tuning selection pressures.

## 195 Technical requirements

196 To implement the above considerations, it was critical to make cell proliferation fully dependent on
197 the POI's 1-0-1-0-… output. The key idea was to find a gene, which would be required for one step in
198 proliferation but block another (Fig. 1 B-D). By engineering the POI to fully control this element, the
199 POI would drive one cell cycle for each 1-0 output oscillation of the POI.

200 The overall system needed to satisfy stringent requirements:

201 1. Tight coupling: Each proliferation step must be tightly dependent on the switching of the POI.
202 Mutations that turn the POI constantly on (1) or off (0) should block cell proliferation (Fig. 1 D).

203 2. Mutational robustness: No (known) mutations should break the tight coupling of the POI and
204 cell proliferation. Such mutations would otherwise allow bypassing the selection pressure.

205 3. Reliability: A brief period of the POI's 1 output should trigger one step in cell proliferation in
206 most cells, and switching to 0 should allow the completion of the rest of a proliferative cycle.
207 Repetitive 1-0 switches at the right times should drive cells through consecutive growth-division
208 cycles.

209 4. Tolerance to poor initial performance: POIs may work too poorly to drive the system initially.
210 Genetic constructs, which we call 'training wheel plasmids', should support cell proliferation initially
211 and should be cleanly removable early in the directed evolution campaign.

212 5. Usability: Any POI should be easily insertable in a plug-and-evolve fashion.

213 6. Stability: Over long periods of directed evolution, cells should maintain a stable genome and
214 not polyploidize, which makes genetic analyses difficult.

## 215 Implementation in budding yeast

216 We engineered the system in budding yeast because it has a relatively fast cell cycle (≈90 min period
217 in glucose medium), which has been researched extensively. A short generation time is important
218 since it sets the maximum speed with which selection pressure can be exerted on POI state switching.

219 In search of a gene that is essential or poisonous for different proliferative steps, one might consider
220 cell cycle control regulators, which oscillate once per cell cycle. However, it is not obvious which to
221 choose since the cell cycle control system is remarkably robust. For example, constitutive expression
222 of *CLN2* and *CLB2* in the absence of all other Cdk1 cyclins (*cln1-3Δ clb1-6Δ*) suffices for cell cycles[83].
223 Even in such a highly stripped-down cell cycle control system, the remaining two Cdk1 cyclins do not
224 need to oscillate transcriptionally.

225 However, past experiments showing that constant transcriptional induction suffices for cell
226 proliferation were often performed with relatively weak promoters such as *GALL*[55]. Thus, we pursued
227 a strategy, in which we re-examined elements of cell cycle control for their potency, that is, being
228 essential for one part of the cell cycle but poisonous for another, at least, when over-expressed. Once
229 found, we could engineer cells to be even more sensitive to both the need for the cell cycle regulator
230 at one cell cycle stage and poisonous for the other.

231 For our search, we used the relatively strong blue-light-induced LOV transcription factor El222 and the
232 El222-controlled *LIP* (**Supplementary Note 1**). This system allowed us to test rapid switches in glucose
233 medium, where proliferation is relatively fast. We transformed yeast with constructs, in which *LIP*
234 controlled the transcription of cell cycle regulators we wished to test (Table 1, column 1). In these
235 cells, we had deleted endogenous cell cycle control genes whose absence makes the corresponding
236 inducible cell cycle gene essential. Further, cells were kept viable before our tests by inducible

237 transcriptional constructs that could be shut off for the test (Table 1, column 2). For more details on
238 cell cycle regulation in budding yeast generally or in our final strain, see **Supplementary Note 2**.

| Candidate cell cycle regulator controlled by El222/*LIP* | Genetic background for tests | Result |
|---|---|---|
| *CLB2* | *clb1,2Δ*<br>*GALL-CLB2* | Constitutive overexpression failed to arrest cell cycle |
| *CLB2kdΔ* | *clb1-6Δ swe1Δ*<br>*GALL-CLB2* | Pulsatile expression regime could not be found for continuous cell cycles |
| *CDC20* | *cdc20Δ, cdh1Δ*<br>*MET3pr-CDC20* | Constitutive overexpression failed to arrest cell cycle |
| *CLN2* | *cln1-3Δ*<br>*MET3pr-CLN2* | Constitutive overexpression failed to arrest cell cycle |
| *CLB5* | *cln1-3Δ*<br>*MET3pr-CLN2* | Oscillatory induction needed for cell cycles |
| *CLB5* | *cln1-3Δ clb3,4,6Δ*<br>*MET3pr-CLN2* | Oscillatory induction needed for cell cycles |

239 Table 1: Tests to identify cell cycle regulators which are needed for one part of the cell cycle but toxic
240 for another in specially engineered genetic backgrounds. During the tests, we turned off the chemical-
241 responsive promoters *MET3pr* and *GALL*.

242

243 We tested for three different properties: inviability given continuous off (0) or on (1) expression as
244 well as proliferation under periodic expression. We started with the key components of the core
245 cyclin-Cdk/APC negative feedback loop of the cell cycle (Table 1, Fig. 2 A). First, we tested optogenetic
246 control of *CLB2*, the major M cyclin in budding yeast[84], in a *clb1,2Δ* background. As expected, in
247 darkness, the lack of *CLB1* and *CLB2* caused cells to arrest before mitosis. However, continuous
248 expression of *LIP-CLB2* did not prevent cells from cycling in glucose medium, contrary to our
249 expectations based on strong, multi-copy *GAL1pr-CLB2* over-expression in galactose medium[85,86].
250 Since Clb2 activity has to be reduced in order to allow cell cycle exit, we next tested whether Clb2kd,
251 an undegradable variant of Clb2 was more suitable. Clb2kd continued to be needed for entry into
252 mitosis and anaphase in a *clb1,2Δ* background. However, we could not find a regime of pulsing light
253 under which cells performed continuous cell cycles. After a few cell cycles, Clb2kd blocked mitotic exit
254 nearly permanently presumably because Sic1 inhibition and dilution did not reduce Clb2kd
255 concentrations sufficiently. In previous work, budding yeast cells had been shown to be very sensitive
256 to the duration and period of joint Start cyclin and *GAL1pr-CLB2kd* pulsing over only a few cell cycles,
257 which was interpreted as a signature of an artificial incoherent feedback loop which had been

258 incorporated into cell cycle control[87]. Next, testing the B-type cyclin antagonist *CDC20*, whose
259 deletion leads to metaphase arrest, we found that it was similarly not suitable since *LIP-CDC20*
260 overexpression did not arrest cells.

261

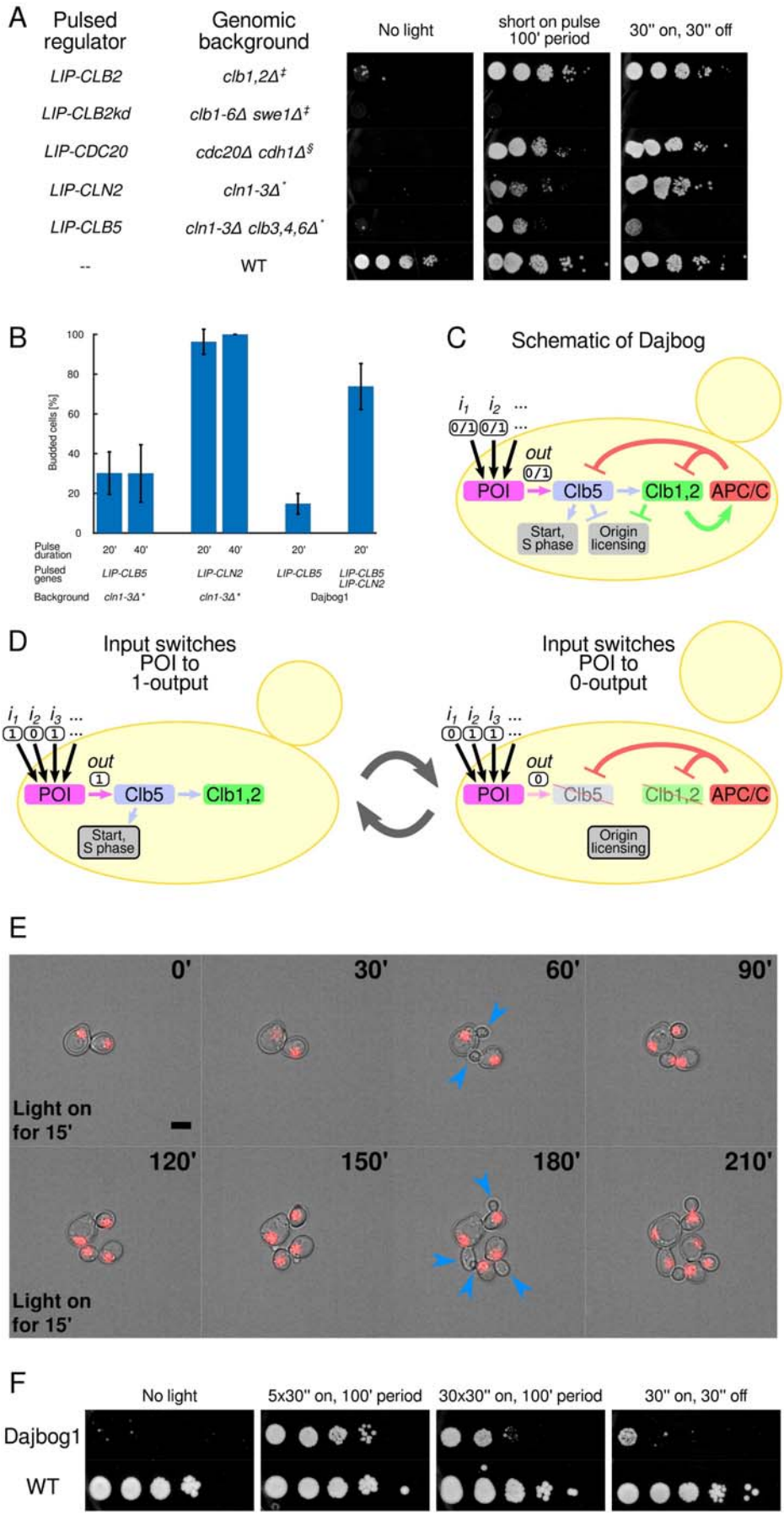
A
Pulsed regulator
Genomic background
No light
short on pulse 100' period
30'' on, 30'' off
LIP-CLB2
clb1,2Δ‡
LIP-CLB2kd
clb1-6Δ swe1Δ‡
LIP-CDC20
cdc20Δ cdh1Δ§
LIP-CLN2
cln1-3Δ*
LIP-CLB5
cln1-3Δ clb3,4,6Δ*
--
WT
B
Budded cells [%]
Pulse duration
Pulsed genes
Background
cln1-3Δ*
Dajbog1
C
Schematic of Dajbog
POI
Clb5
Clb1,2
APC/C
Start, S phase
Origin licensing
D
Input switches POI to 1-output
Input switches POI to 0-output
E
0'
30'
60'
90'
120'
150'
180'
210'
Light on for 15'
F
No light
5x30'' on, 100' period
30x30'' on, 100' period
30'' on, 30'' off
Dajbog1
WT

262

263 Figure 2. Engineering budding yeast strains for optovolution. A: Initial tests of different cell cycle regulators with respect to
264 three properties: essential for proliferation (cells inviable when regulator is off), sufficient for proliferation when pulsed (5
265 light pulses of 30 sec on, 30 sec off administered every 100 min, except for *cln1-3Δ clb3,4,6Δ* we used 30 such light pulses),
266 and lethal when expressed continuously (30 sec on, 30 sec off). All cells expressed *EL222*, which induces *LIP*. (Note that
267 panel F shows tests for the Dajbog1 strain, which has been improved with respect to these desired properties.) B:
268 Efficiency of cell cycle initiation (budding) when different light-inducible cell cycle regulators are activated, assessed by
269 timelapse microscopy. Error bars show 5-95% confidence intervals. Number of scored cells are given in the Supplementary
270 Table 3. C: Schematic of cell cycle regulators in Dajbog strains. A subset of key cell cycle elements is shown only. Cln2 and
271 Sic1 were omitted for clarity. D: Illustration of cell cycle states of the Dajbog strains when the POI output is on (1) or off
272 (0). E: Timelapse recording of Dajbog1 strain, exposed to diascopic microscope light every 120 min for 15 min. Cells carry
273 the red fluorescent nuclear marker Htb2-mCherry. Scale bar: 5 µm. F: Spot test of Dajbog1 strain under different light
274 pulse regimes, revealing 5 times 30 sec on, 30 sec off every 100 min to be optimal among the conditions tested. To keep
275 cells proliferating before the tests, cells carried chromosomal constructs with chemical inducible *MET3pr-CLN2* (*), *GALL-*
276 *CLB2* (‡), or *MET3pr-CDC20* (§), which were shut off during the tests by glucose or methionine in the agar plates.

277

278 The cell cycle regulators discussed thus far control mitotic transitions, where arrest and release often
279 induces aneuploidy. We next shifted our focus to cyclins which control the G1-to-Start transition,
280 which is less perilous for genomic stability. Parameters and response signatures of *CLN2* pulsing were
281 extensively tested in ref.[87] However, again, constitutive over-expression of the G1/S cyclin *CLN2* from
282 El222/*LIP* in the *cln1-3Δ* background, where *CLN2* is essential, did not kill cells. Thus, we turned to the
283 S-phase cyclin *CLB5*. We first tested *LIP-CLB5* in a *cln1-3Δ* strain since *CLB5* expression is known to
284 override a *cln1-3Δ* G1 arrest, although with lower efficiency than G1/S cyclin *CLN2*. In darkness, cells
285 were arrested in G1. Light pulses with a 90 min period led to repeated cell cycles. Fortuitously, we
286 found that constitutive *CLB5* expression by El222/*LIP* was lethal. (In contrast, *GAL1pr-CLB5*
287 overexpression in galactose medium, as opposed to glucose medium, where cell cycles are
288 substantially slower, is tolerated.) Thus, *CLB5* was a promising candidate for creating a tight coupling
289 between the POI and the cell cycle. The system fulfilled requirement 1.

290 Next, we engineered the system for mutational robustness (requirement 2). To further increase the
291 cells' dependence on *LIP-CLB5* expression, we deleted the four chromosomal *CLB3,4,5,6* genes, which
292 can be functionally redundant with light-induced *CLB5*[88,89]. No mutations are known that can by-pass
293 the requirement for Clb5 in a *cln1-3Δ clb3-6Δ* background.[90]

294 By deleting *CLB3-6* to make the strain even more strongly depend on *LIP-CLB5* induction, we could
295 next also make the strain less tolerant to continuous *LIP-CLB5* expression. This would further increase
296 the need for Clb5 to oscillate on and off for proliferation. We accomplished this by deleting *SIC1*, a B-
297 type cyclin inhibitor. *SIC1* is part of a circuit that can oscillate when cyclin levels are constant, thus
298 rescuing such cell cycles[83]. When *SIC1* is deleted, the *cln1-3Δ* arrest becomes leaky[91]. However, we

299 found that this depends on at least one of the *CLB3-6* genes being present. *cln1-3Δ clb3-6Δ sic1Δ* cells
300 continued to be tightly blocked in darkness.

301 The reliability of cell cycle initiation in response to a *LIP-CLB5* pulse was low (Fig. 2 B), violating
302 requirement 3. Only 30% of *cln1-3Δ* cells budded in response to a LIP-CLB5 pulse. In *cln1-3Δ clb3,4,6Δ*
303 cells, light-induced *LIP-CLB5* led to budding in even fewer (15%) of G1-arrested cells. This fraction was
304 much higher (>90%) for *cln1-3Δ* cells with *LIP-CLN2*. Increasing the duration of the light pulse did not
305 change the fraction of *cln1-3Δ* cells that committed to the cell cycle. Guided by these results, we
306 sought to increase the reliability of the response to light pulses by adding a *LIP-CLN2* construct. This
307 does not undermine the dependence on *LIP-CLB5*, which continues to be essential for S phase and
308 triggering entry into mitosis in the *cln1-3Δ clb3-6Δ* background. Simultaneous expression of *LIP-CLN2*
309 and *LIP-CLB5* in the *cln1-3Δ clb3,4,6Δ* background led to a more reliable >70% of cells budding in
310 response to a 20 min pulse of light, satisfying requirement 3.

311 To enable routine propagation of these cells prior to directed evolution campaigns, we created a
312 'training-wheel plasmid' (requirement 4). This plasmid allowed cells to grow without exogenously
313 induced Clb5 oscillations, and the directed evolution begins with counter-selection against this
314 plasmid. We used a *URA3*-marked CEN/ARS plasmid, which can be selected against with 5-FOA,
315 containing a *CLB5* copy and *MET3pr-CLN2*. Finally, to increase the mutation rate for directed
316 evolution, we introduced the *pol3-L523D*[92,93] mutation that is reported to increase the global
317 mutation rate about one-hundred fold.

318 In summary, we achieved tight coupling of the cell cycle machinery to externally applied periodic on-
319 off light signals using Clb5 (aided by Cln2) in a *cln1-3Δ clb3-6Δ sic1Δ* background (Fig. 2 C-F). Clb5
320 triggered Start, S phase, and mitotic entry (Fig. 2 D). Simultaneously induced Cln2 substantially
321 increased the fraction of cells initiating a cell cycle in response to a pulse of light. Once Clb5 and Cln2
322 are no longer induced, they are degraded and diluted, allowing completion of each cycle and resetting
323 the cell state for a new cycle. In darkness or low light, cells arrested in G1. Under constant light, cells
324 could not proliferate as expected due to Clb5 blocking origin of replication relicensing[94,95]. The
325 poisonous effect of Clb5 can be enhanced by the *SIC1* deletion[96]. We further increased the mutation
326 rate globally with the *pol3-L523D* mutation[92]. Also, we allowed the strain to proliferate without Clb5
327 oscillations using a training wheel plasmid until the start of each directed evolution campaign. In
328 principle, any POI controlling Clb5 activity can be inserted for directed evolution (requirement 5). In
329 our tests, we never found strains to polyploidize, allowing straightforward genetic analysis if needed
330 (requirement 6). The strain fulfilled the requirements for the evolution of dynamic, multi-state, and
331 computational protein functionalities. We named the strain Dajbog2, and also used a variant with
332 wild-type *SIC1* when more tolerance to POI leakiness was required, which we named Dajbog1.[97]

333 Independently of the use for directed evolution, researchers have previously aimed to entrain the cell
334 cycle-clock to external pulses of a chemical or light. To our knowledge, this is the first case where the
335 cell cycle is slave to external signals in an evolutionary robust manner.

## 336 Directed evolution of a LOV-transcription factor

337 The Dajbog strains can in principle be used for generally evolving dynamic, multi-state, and
338 computational functionalities. We first applied the method to optogenetic systems. Thus, the POI was
339 the light-sensitive protein. Optogenetic systems relay external on (1) or off (0) light states to on (1) or
340 off (0) cellular activity, i.e., they have two input-output relationships. Optogenetic systems have been
341 challenging to evolve, requiring repeated, sequential campaigns for the on (1) and off (0) output
342 states since mutations improving one output state may destroy the other. Given that El222 is itself
343 widely used and that LOV domains are of broad interest, we chose to evolve El222 toward i) greater
344 light sensitivity, ii) less leakiness, or iii) different excitation spectra for multiplexing and reduced
345 phototoxicity.

346

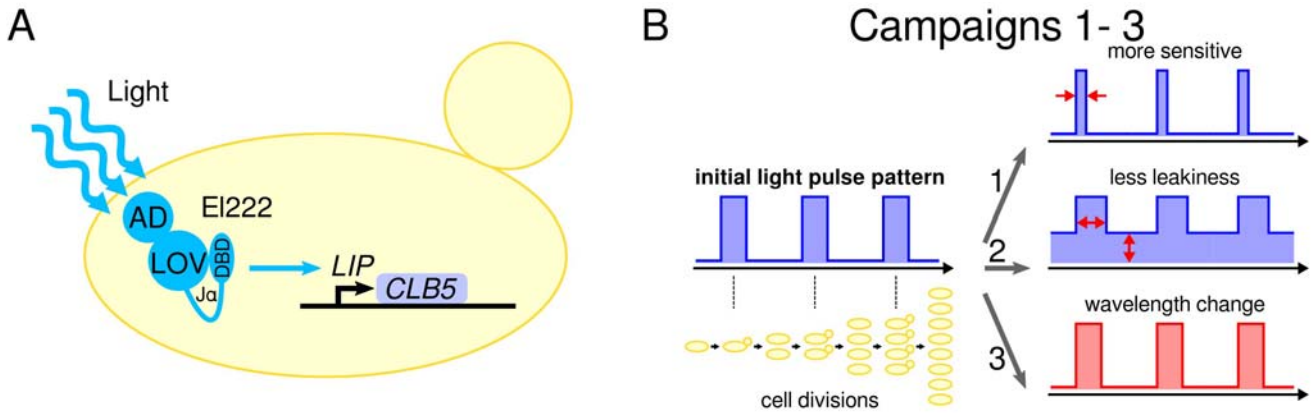


347

348 Figure 3. Directed evolution campaigns 1-3 with LOV-transcription factor El222 as POI. A. Schematic of wiring diagram for
349 El222 evolution. *CLN2* and other cell cycle regulators omitted for clarity. AD, activation domain; LOV, LOV domain; Jα, Jα
350 helix; DBD, DNA binding domain. B. Schematic of three directed evolution campaigns. The initial light pulse pattern was
351 switched to 1) very brief pulses, 2) long pulses with additional ambient light, or 3) green and red light pulses. Under these
352 latter conditions, wild-type Dajbog cells did not proliferate.

353

354 We used the Dajbog strains with El222 directly controlling *CLN2* and *CLB5* transcription in the same
355 configuration as for testing and developing our method (Fig. 3 A). Cells initially proliferated under a
356 permissive light pulse regime (5 times 25 sec on, 35 sec off every 100 min). Then, we changed the
357 light pulse regime to apply specific selection pressures, in which cells with wild-type El222 could not

358 proliferate (Fig. 3 B). (See Supplementary Fig. 1 for the excitation and imaging light spectra.) With cells
359 spread on agar plates, colonies emerged after about two days.

360 After evolution, we cloned the mutated *EL222* gene and introduced it as a single copy in wild-type
361 budding yeast cells where *LIP* drives the transcription of the bright, yeast-optimized *yEVenus*
362 fluorescent protein gene. Thus, potential mutations elsewhere in the genome of the Dajbog cells,
363 which could have emerged in the directed evolution campaign, could not affect our characterizations
364 of the El222 variants. For timecourse measurements, where the dynamic nature of the reporter is
365 important, we used yEVenus tagged with a PEST degron to reduce the fluorescent protein's half-life[82].
366 We took fluorescence microscopy images and processed them using YeaZ, a deep neural network for
367 analyzing yeast images.[98] This approach ensured higher accuracy compared to fluorescence
368 quantification by flow cytometry, for example[55]. We express all levels in maxGAL1 units, i.e., the
369 maximum expression level of the same fluorescent reporter when driven by the *GAL1* promoter in
370 galactose medium, an easy-to-communicate, intuitive unit for transcription. We thus followed the
371 same method of characterization as was used for benchmarking inducible transcriptional systems in
372 ref.[55]

373 In the first directed evolution campaign, we sought to enhance the 1-output (on) state of El222. This
374 would allow higher output under low light conditions. To evolve more light-sensitive mutants, we
375 exposed cells to very brief light pulses (1 sec on every 100 min, Fig. 3 B). In the colonies that grew
376 under these conditions (Fig. 4 A), we found 11 different El222 mutations (Fig. 4 B). Remarkably, using
377 Dajbog2 (with *sic1Δ*) we observed 96% (n = 247) of colonies had a mutation in *EL222* while Dajbog1
378 (with *SIC1*) permitted mutations elsewhere in the genome to rescue cells (10% in *EL222*, n = 816). The
379 new El222 variants showed improved light sensitivity, with levels of transcription under low-intensity
380 light up to 16 times higher than with wild-type *EL222*. Several variants were comparable or more light
381 sensitive than the most sensitive El222 mutant to date, strongLOV, which we had engineered
382 previously[55].

383 To characterize the dynamic properties of the evolved El222 variants, we monitored their activity by
384 fluorescence timelapse microscopy where we induced them with diascopic light for 3.5 h (Fig. 4 C). All
385 tested variants showed increased activity compared to wild-type El222 when using a constant light
386 source of 8.4 mW/cm$^2$. For most variants, we observed a trade-off between strength and turn-off
387 dynamics, similar to strongLOV[55]. However, remarkably, the highly light-sensitive variant A157V,
388 containing a mutation in the Jα helix, showed turn-off dynamics comparable to wt-El222. (All
389 references to mutant residue numbers in El222 are conventionally given with respect to bacterial
390 El222 system to match the numbering used in previous work[55,99,100]).

This mutant is further interesting because it is the only one outside the LOV domain of El222 (Fig. 4 D). Within the LOV domain, the Fα helix, which is adjacent to the chromophore, proved to be particularly enriched for light-sensitizing mutations.

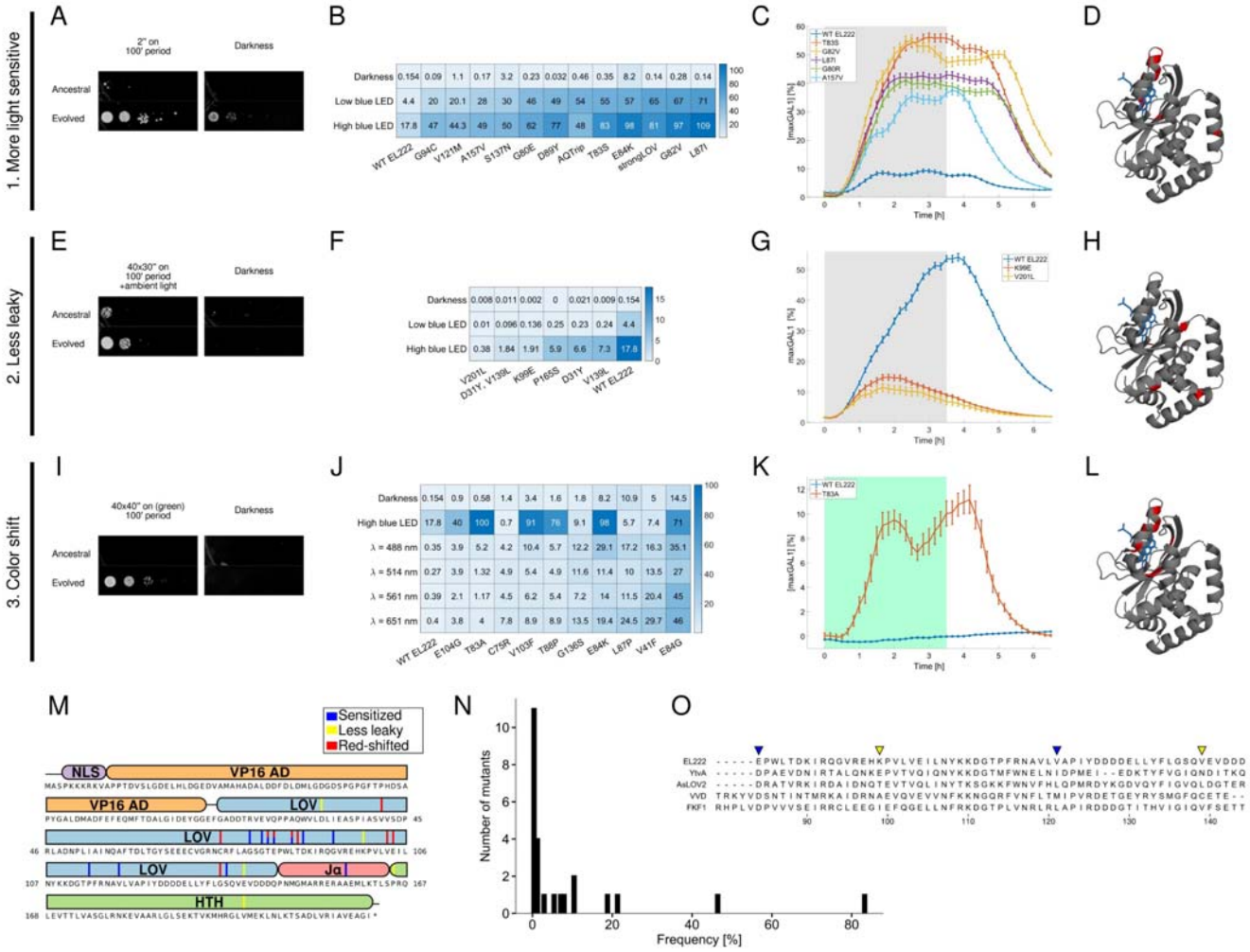


Figure 4. Results of three directed evolution campaigns of El222. Directed evolution for higher light sensitivity (A-D), lower leakiness (E-H), and color shift (I-L). Panels A, E, I represent spot tests for the wild-type Dajbog strain (ancestor) and typical mutants (evolved) that emerged in the different campaigns. Panels B, F, J show *in vivo* steady-state expression levels of mutant El222 driving a transcriptional fluorescent reporter under different light exposure conditions. All values are in maxGAL1 units[55]. In panel B, we included AQTrip[100] for reference. C, G, K show timecourses of some of the El222 mutants we characterized, driving a destabilized fluorescent transcriptional reporter with PEST degron. The optogenetic systems were induced from 0 h to 3.5 h by diascopic light (C, G) or with an additional green filter inserted into the light path (K) as indicated by the highlighted region[55]. Error bars show the standard error of the mean around each timepoint. Panels D, H, K depict the locations of the mutations (red) in the dark-state 3D structure of El222 (PDB ID: 3P7N)[99]. M: Positions of mutations in domain diagram of El222. N: Histogram of the frequency with which the mutations from our three campaigns are found in putative LOV domains identified in ref.[101]. O: Searching for the mutations from our three campaigns in LOV domains with characterized dark-reversion kinetics[56] (FKF1 from *Arabidopsis thaliana*, VVD from *Neurospora crassa*, YtvA

408 from *Bacillus subtilis*, and the LOV2 domain of phot1 from *Avena sativa*) identifies the light-sensitizing V121M and
409 strongLOV (E84D) mutations (blue arrows) and the mutations K99E and V139L (yellow arrows), which reduce leakiness. All
410 references to mutant residue numbers in El222 are given with respect to bacterial El222, to match the numbering used
411 previously[55,99,100]. B, C, F, G, J, K: Numbers of analyzed cells are given in the Supplementary Tables 4-7. All measured
412 characteristics of the new El222 mutants have been added to the Inducible Transcriptional Systems Database
413 (https://promoter-benchmark.epfl.ch/)[55].

414

415 In the next campaign, we sought to reduce the leakiness of El222, that is, suppress activity in the 0-
416 output (off) state. This is particularly important for applications where background expression needs
417 to be minimized, e.g., when controlling toxic genes. We exposed cells to very long duration pulses of
418 light (40 times 30 sec on, 30 sec off every 100 min, Fig. 3 B) in addition to continuous, dim background
419 light (Fig 4 E-H). This was lethal to the Dajbog strain with wt-El222 (Fig. 4 E). We identified five new
420 mutations whose leakiness was nearly indistinguishable from levels of background transcription from
421 *LIP* in the absence of El222 (Fig. 4 F, Supplementary Fig. 2). As expected, they were also overall less
422 strongly induced by light. One of the colonies that emerged had fixed two mutations in the LOV
423 domain (D31Y, V139L). To understand their individual contributions to the phenotype, we tested
424 them separately. The mutations contributed independently and about equally under high blue LED
425 light. We also measured the on-off dynamics of low-leakiness mutants by fluorescence microscopy.
426 Using continuous light of 8.4 mW/cm$^2$ as in the case for light-sensitized mutants led to no observable
427 activity in the low-leakiness mutants (not shown). Under stronger light (97 mW/cm$^2$), the mutants
428 responded at 20% of wt-El222 output (Fig. 4 G). The low-leakiness mutations were both in the LOV
429 domain as well as the DNA binding domain (Fig. 4 H).

430 The number of low-leakiness mutants that we discovered in the second campaign was smaller than
431 the number of light-sensitized mutants we found in the first campaign. We speculate that this is due
432 to the LOV domain of El222 having a relatively fast off rate of 30 sec, substantially faster than many
433 previously characterized LOV domains[54,56]. Thus, there may exist few opportunities for speeding up
434 the off kinetics further without destroying function.

435 In our third campaign, we sought to modify the nature of the 1-output state with respect to color
436 responsiveness. We switched Dajbog cells from growing under only blue light pulses to green, orange,
437 and red light combined (40 times 30 sec on, 30 sec off every 100 min). (Figs. 3 B, 4 I-L, Supplementary
438 Fig. 1 for details regarding light sources). We discovered numerous mutations in El222 that allowed
439 colonies to grow under these light pulses. Again, optovolution was highly efficient: 96% (n=247) of
440 mutations were in the *EL222* ORF when Dajbog2 (with *sic1Δ*) was used and 10% (n = 816) with
441 Dajbog1 (with *SIC1*).

442 Since the green LEDs that we used had an emission spectrum that extended below 500 nm
443 (Supplementary Fig. 1), which overlaps with the excitation spectrum of wt-El222[99], we next excluded
444 merely light-sensitized mutants with a 514 nm laser. Ten El222 mutants showed substantial
445 transcription when excited by a 514 nm laser (Supplementary Fig. 3). We focused only on these
446 mutants and disregarded the others. To measure the *in vivo* action spectrum of the mutant El222s,
447 that is, the relationship between the wavelength of excitation light and the level of activity, we used
448 additionally blue 488 nm, yellow 561 nm, and red 651 nm lasers (Fig. 4 J). To detect the sensitivity to
449 each wavelength and not saturate the on (1) state of the transcription factors, we set the lasers to
450 relatively low average power (3.5 mW/cm$^2$ delivered over 6 h), which was enough to induce all of the
451 color-shifted mutants. We also included as a reference the blue LED light used for characterization of
452 the previously described sensitized and low-leakiness variants (Fig. 4 B, F). The measurements (Fig. 4
453 J) showed that the mutated El222 variants were not only responsive to green but also to red light. In
454 fact, red 651 nm laser light generated comparable or even stronger responses from our color-shifted
455 El222 variants. Some of the variants responded to red light much more strongly than wild-type El222
456 to blue light but were also more leaky. The largest dynamic range we observed was 7.5x for the G136S
457 mutant. Surprisingly, under blue light of high intensity, some of the mutants (C75R, G136S, L87P, and
458 V41F) showed lower level of activity compared to blue or red laser light of low intensity. We
459 characterized the dynamics of a red-shifted mutant using fluorescence microscopy and a *LIP-*
460 *ymScarletI-PEST* reporter (Fig. 4 K).

461 While for the light-sensitized and low-leakiness variants, the mutations were mostly away from the
462 photoreceptive core, the red-shifted mutations clustered tightly around the chromophore (Fig. 4 L).
463 Interestingly, one of the red-responsive variants had an arginine residue instead of the critical Cys-75
464 residue that forms a covalent bond with the chromophore after exposure to blue light[102]. In *in vitro*
465 experiments, LOV domains without this strictly conserved cysteine were previously shown to
466 incorporate a partially reduced flavin chromophore[103], pointing to one potential explanation for our
467 color-shifted El222 mutants.

468 In total, we discovered 25 mutations, mostly in the LOV domain, 1 in the Jα helix, and two in the DNA
469 binding domain (Fig. 4 M).

470 LOV domain proteins such as El222 are ubiquitous across the tree of life and control a variety of
471 cellular processes. Most approaches to altering LOV-optogenetic tools have involved introducing
472 mutations from other known natural LOV domains, which were faster or slower cycling[54,56,100]. To
473 gauge how realistic it would have been to discover our evolved mutants rationally, we first quantified
474 the novelty of our mutants by searching a catalog of 7000 known and putative LOV-domains (Fig. 4 N)
475 as well as by aligning their sequences with the well-studied LOV-domain proteins FKF1 from
476 *Arabidopsis thaliana*, VVD from *Neurospora crassa*, YtvA from *Bacillus subtilis*, and the LOV2 domain

477 of phot1 from *Avena sativa* (Fig. 4 O). We discovered that the majority of the mutations (21/25) were
478 rare (≤10%) in putative LOV domains, and 4 are present in LOV domains whose kinetics had
479 previously been characterized. V121M found in VVD is part of the rationally-designed El222 variant
480 AQTrip[100]. Similarly, another mutation (E84D) was used to construct the more light-sensitive
481 strongLOV mutant protein by us recently (Fig. 4 O, blue triangle). Interestingly, the other two
482 mutations, K99E and V139L (Fig. 4 O, yellow triangles), would have been expected to lead to more
483 stable light-adapted states based on previously measured off-kinetics[54] but we found them, instead,
484 to lead to lower leakiness and overall weaker responses. These findings further underscore the power
485 of directed evolution for identifying functional mutations with specific desired properties.

## 486 Long-term optovolution of light-sensitized LOV domains

487 The directed evolution campaigns described thus far were unbiased by design: Any El222 mutant
488 which emerged and which could switch on and off repeatedly for ≈2 days under the respective
489 selection pressure would generate a colony and be detected by us. Next, we wished to test whether
490 optovolution could be used for directed evolution over longer periods of time in liquid culture, where
491 mutations could compound and compete against one another. The fittest mutant would take over the
492 cell culture.

493 We again sought to boost the 1-output activity of El222, this time over one week (**Methods**). We
494 evolved the Dajbog2 strain under 5 sec of light, administered every 100 min. We observed two
495 mutations that won in two different long-term experiments, E84D and V121M, which we had already
496 discovered using the previous unbiased approach.

## 497 Comparison with the -Ura/+FOA method

498 We wished to compare optovolution to other approaches that have been pursued for evolving multi-
499 state proteins, which rely on sequential directed evolution campaigns for each of the POI output
500 states. Note that in optovolution, alternating selection for the 0- and 1-output states as well as for
501 switching back and forth occurs once per cell cycle every ≈90 min. The -Ura/+FOA system represents a
502 reasonable comparison for optovolution since it requires input-dependent proliferation under two
503 opposite selection pressures: growth requires induced expression of *URA3* in -Uracil medium and
504 suppression of *URA3* in 5-FOA medium. This method was used in the directed evolution of the CRY2-
505 CIB optogenetic system.[27]

506 For this comparison, we constructed a budding yeast strain in which *URA3* is induced by the El222/*LIP*
507 system in a genetic background where the endogenous *URA3* ORF was deleted (Fig. 5). We validated
508 the *LIP-URA3* construct by confirming that the cells were dead in -Uracil (absence of Uracil) medium in
509 darkness and viable in -Uracil medium under 30 sec on, 30 sec off pulsing blue light. However, cells

510 were also dead in 5-FOA medium in darkness, presumably due to the leakiness of El222/*LIP*. (Note
511 that we had already sought to minimize leakiness by inserting the *LIP-URA3* construct and *EL222* gene
512 as single copies.) *URA3* codes for orotidine 5′-phosphate decarboxylase, which is a highly proficient
513 enzyme[104], potentially explaining how even low basal transcription may not be tolerated in 5-FOA
514 medium.

515 Because the counter-selection step for low 0-output (off) activity did not yield any surviving mutants,
516 we did not work to boost the 1-output (on) state of El222. Instead, we sought to leverage this
517 sensitivity to 0-output activity to evolve less leaky El222. We selected for *LIP-URA3 PGK1pr-EL222*
518 *ura3Δ0* cells that grew on 5-FOA in darkness. However, after sequencing 200 strains that were
519 resistant to 5-FOA, we could not find mutations in *EL222*. Instead, as expected, some strains had
520 mutations in the *URA3* gene. Because there was no selection pressure for *URA3* function, it could
521 simply be corrupted. Such by-pass of the selection pressure by loss-of-function of the POI is
522 fundamentally impossible in optovolution by design.

523

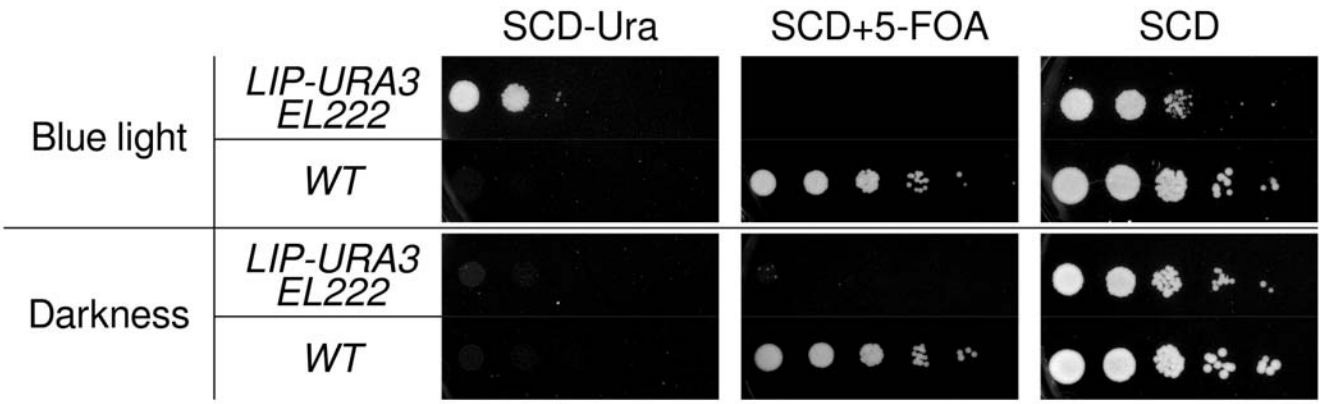


524

525 Figure 5. Challenges of using the -Ura/+FOA method for the directed evolution of El222. The test *ura3Δ0* strain carried
526 single copies of *LIP-URA3* and *PGK1pr-EL222* constructs. The control strain was wild-type W303, which is auxotrophic for
527 uracil. Because of the inviability of the test strain in darkness on +5-FOA, we could not perform light-sensitization
528 campaigns. On the other hand, none of 200 mutant colonies that emerged under these conditions had mutations in *EL222*
529 so that the opposite campaign for low-leakiness mutants also failed.

530

## 531 Directed evolution of the PhyB-Pif3 system independent of exogenous chromophore

532 In our next evolutionary campaign, we wished to improve the usability of the red-/far-red-light
533 controlled optogenetic switch PhyB-Pif3. For this purpose, we put *CLN2* and *CLB5* under the control of
534 the *GAL1* promoter and introduced *ADH1pr-PHYB-GAL4BD* and *ADH1pr-GAL4AD-PIF3* circuits. (Fig. 6
535 A). We screened for mutations allowing cell proliferation without supplementing PCB (Fig. 6 B).

536 We found mutations in the *YOR1* (also known as *YCF1*) gene, two of which were early nonsense
537 mutations (Q64*, E421K, E1318*). Yor1 is a plasma membrane exporter[105], a homolog of human cystic
538 fibrosis transmembrane receptor (CFTR)[106], which may prevent the accumulation of a cellular
539 metabolite with PCB-like tetrapyrrole structure. To test that PhyB-Pif3 functioned due to loss-of-
540 function of *YOR1*, we deleted *YOR1* in a strain from ref.[76], in which PhyB-Pif3 drives the transcription
541 of a fluorescent reporter (Fig. 6 C). In the absence of PCB, the strain with *YOR1* deletion responded
542 similarly as with PCB in the presence of *YOR1*. Leakiness was comparable with and without *YOR1*.

543 Since PhyB-Pif3 is frequently used to control localization of proteins to different cellular
544 compartments, we tested that *yor1Δ* sufficed to replace supplemental PCB for this purpose as well.
545 We deleted *YOR1* in a yeast strain from ref.[107] in which PhyB is anchored to mitochrondria, labeled
546 with mCherry, and Pif3 is fused to a yellow fluorescent protein and Bem1 (PhyB-mCherry-Tom7,
547 Bem1-mCitrine-Pif3). Exposing the *yor1Δ* version of this strain to red light led to colocalization of PhyB
548 and Pif3, indicating their interaction (average per-cell Pearson correlation for yellow and red
549 fluorescence r = 0.60, N_cells = 21). As a control, we tested the colocalization of PhyB and Pif3 in
550 *yor1Δ* strain with PCB, which led to r = 0.73 (N_cells = 32). In wt-*YOR1* cells we observed low
551 colocalization (r = 0.25, N_cells = 17), while the addition of PCB to showed localization extent
552 comparable to *yor1Δ* without PCB (r = 0.78, N_cells = 31).

553

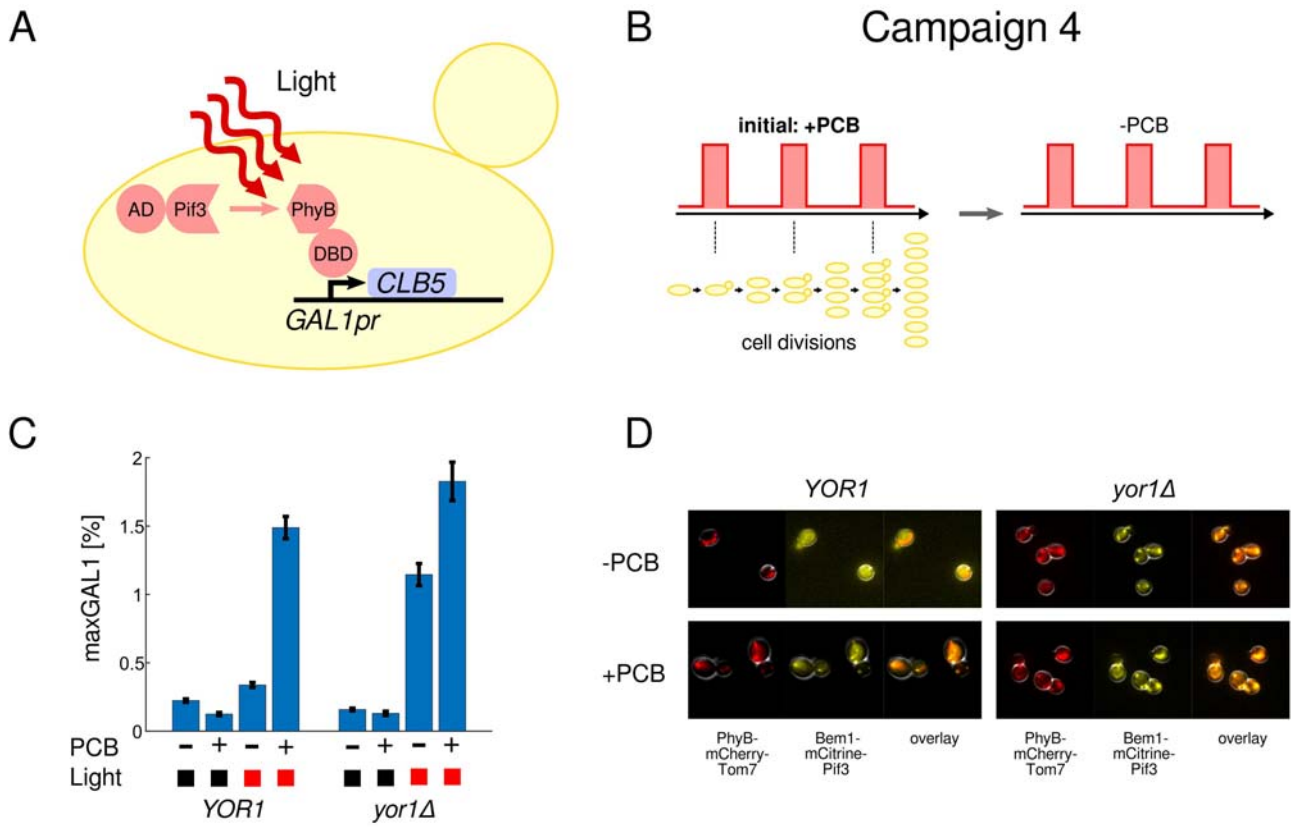


Figure 6. Directed evolution campaign 4 to lose the dependence of PhyB-Pif3 on PCB. A: Schematic of wiring diagram relevant for campaign. (CLN2 and other cell cycle regulators omitted for clarity.) AD, activation domain; DBD, DNA binding domain. B: Schematic of campaign. C: GAL1pr-yEVenus induction with or without YOR1 deletion, which was identified in this campaign. Error bars represent standard error of the mean. Numbers of analyzed cells are given in Supplementary Table 8. D: Test of co-localization of Pif3 to mitochondrially anchored PhyB with or without YOR1. The PCB concentration was 10 µM where supplemented. The measured characteristics of PhyB-Pif3 with and without YOR1 have been added to the Inducible Transcriptional Systems Database (https://promoter-benchmark.epfl.ch/)[55].

## Directed evolution of a light- and doxycycline- inducible AND gate

In our fifth evolutionary campaign, we demonstrate that optovolution can generally evolve dynamic, multi-state, and computational functionalities, not just optogenetic systems. We first engineered an AND gate based on the transcription factor rtTA, which is controlled by doxycycline. To make rtTA dynamically sensitive to transcriptional input, we destabilized it by fusing its N-terminus with a PEST degron. When *PEST-rtTA* was transcribed under the control of the EI222/*LIP* system, transcription from the rtTA-controlled promoter *tetOpr* was very weak.

We wished to evolve variants of the logic gate with stronger on (1) state activity. So, we introduced *tetOpr-CLN2* and *tetOpr-CLB5* into the Dajbog1 strain (Fig. 7 A). We then evolved the system by exposing cells to short pulses of blue light, 2 sec on every 100 min, under which they could not

573 proliferate (Fig. 7 B). Before evolution, light pulsing 30 times 30 sec on, 30 sec off every 100 min and
574 doxycycline allowed cell proliferation, confirming the AND gate functionality prior to directed
575 evolution (Fig. 7 C). However, the *tetO* promoter is very leaky in budding yeast (*tetOpr-yEVenus*
576 expression = 2% maxGAL1 without *rtTA*) so that even in darkness and without doxycycline, Dajbog1
577 proliferated, albeit much more slowly. This is why we used the more leakiness-tolerant Dajbog1 strain
578 in this campaign and screened for mutants as soon as small colonies emerged under 2 sec light pulses
579 every 100 min.

580 In principle, mutations in any part of the system could lead to the increased activity of the on state.
581 Given that we have already extensively characterized the mutations that boost the activity of the
582 El222/*LIP* optogenetic system, we now focused on screening for mutations in *PEST-rtTA*. (While it
583 turned out to be unnecessary here, one can take various measures to minimize the likelihood of
584 mutations in the optogenetic mediator (*EL222*), which would be undesired, versus the POI gene,
585 which would be desired. See **Discussion**.) We discovered two mutations, F67C and R253H (numbering
586 is with respect to +1 methionine in rtTA). To characterize the *PEST-rtTA* mutants, we introduced them
587 as single-copy constructs driven by *PGK1pr* into a reporter strain with a single copy of *tetOpr-yEVenus-*
588 *PEST* (Fig. 7 D). Both mutations showed increased activity in the presence of doxycycline. The mutated
589 residues are located between the DNA binding domain and the rtTA core domain or in the VP16
590 transcriptional activation domain, respectively (Fig. 7 E). Relatedly, in previous directed evolution
591 experiments of rtTA, F67S was identified as increasing the sensitivity of rtTA (without a degron) to
592 doxycycline[108].

593 These results demonstrate how the light-driven selection pressure in optovolution can be leveraged
594 for the evolution of non-optogenetic proteins with dynamic, multi-state, and computational
595 properties.

596

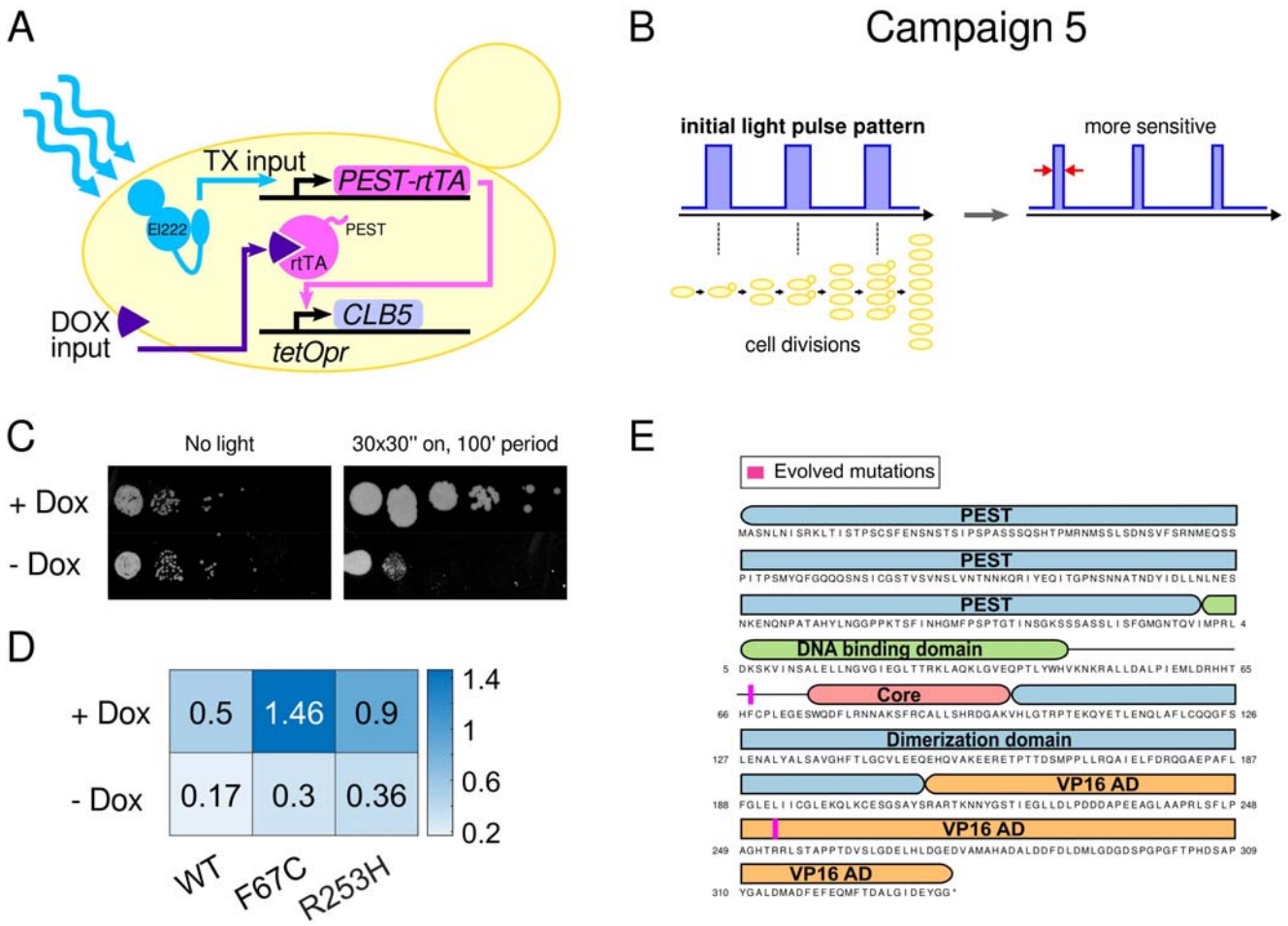


Figure 7. Directed evolution campaign 5 to improve the AND logic gate function of PEST-rtTA. A: Schematic of wiring diagram relevant for campaign. TX, transcription; DOX, doxycycline. B: Schematic of campaign. C: Spot test for wild-type Dajbog1 strain with PEST-rtTA system. D: Expression level of *tetOpr-yEVenus-PEST* under the control of the original or evolved PEST-rtTA in maxGAL1 units. For lowering experimental variability, the original and mutant *PEST-rtTA* were expressed from the *PGK1* promoter. Residue numbers are with respect to +1 methionine of rtTA. Numbers of analyzed cells are given in the Supplementary Table 9. E: Positions of mutations in domain diagram of PEST-rtTA.

## Discussion

Directed evolution is a powerful tool for biological engineering. Given the appropriate selection pressure, directed evolution can solve challenging engineering problems and uncover unexpected solutions -- such as red-responsive El222 mutants or PCB independence conferred by *yor1Δ*. Here, we present the first method that is germane for directed evolution of dynamic, multi-state, and computational protein functionalities. Such capabilities are fundamental to signal transduction -- and thus to life. While much of cellular biochemistry computes decisions, it had been unclear how directed evolution could straightforwardly tune proteins with such capabilities. Apart from interest in

613 this as a fundamental problem, a solution is also needed for protein engineering since dynamic, multi-
614 state, and computational properties are of intense current interest, especially, for protein design[109–
615 113].

616 The limitation we sought to overcome is that current approaches evolve only one functionality at a
617 time. Molecular properties that are not under selection pressure can consequently deteriorate during
618 directed evolution experiments. Not only does the existing work-around for this problem, to run
619 directed evolution campaigns for each functionality sequentially, require repeated interventions and
620 take substantial time[27,29,34], it is also inherently challenging: The basal activity of wild-type El222
621 prevented us from evolving the on (1) output state using the -Ura/+FOA method. Then, in attempting
622 to reduce the leakiness of El222, we did not succeed in finding any mutations in El222 in the two
623 hundred 5-FOA-resistant colonies we tested. Presumably, it was significantly more likely to evolve
624 non-functional mutants than leakiness-reducing mutations. Such likely loss-of-function mutations are
625 not possible with optovolution.

626 Another important feature is that, in contrast to approaches that are not continuous, optovolution
627 obviates manual screening after each round of evolution. In our method, both 0-to-1 and 1-to-0
628 switching of the POI are screened every ≈90 min by the cell cycle control machinery *in vivo*. In
629 addition, the coupling of the desired POI properties to organismal fitness automatically ensures that
630 the evolved variants are functional *in vivo*. Additional *in vitro* screening is not needed. These
631 advantages of our method arise from leveraging cell cycle control, to our knowledge, for the first time
632 for directed evolution.

633 Fundamentally, light control is powerful for directed evolution because it allows communicating with
634 cells rapidly, conveniently, and for extended periods. Thus, new kinds of selection pressures can be
635 created, which require dynamic interaction with cells, as in optovolution. As far as we know, this is
636 the first time that optogenetics has been leveraged for continuous directed evolution.

637 Furthermore, light control allows tuning the fitness landscape of the POI and thus of the selection
638 pressure, enabling different evolutionary outcomes depending on the light protocol. We used the
639 same strain, with El222 directly controlling *CLB5* and *CLN2*, for three different directed evolution
640 campaigns: enhancement of the 1-output activity of El222, suppression of the 0-output activity, or
641 changing the excitation color. However, we only used relatively simple light pulse patterns in this
642 work, that is, we only modified the duration or color of the light pulses (Figs. 3 B, 7 B). By tuning the
643 light pulse parameters further or even combining different pulse types, e.g., long-short-long-short-...
644 light pulses, one may evolve yet more variants of POIs, toward other desirable goals.

645 There is a multitude of possibilities for adjusting the Dajbog strains for different directed evolution
646 campaigns. Decades of research in growth, metabolism, and cell cycle control as well as a large
647 repertoire of tools from yeast genetics can be leveraged:

648 1. The carbon source can be varied to slow down the cell cycle and growth to match POIs that
649 switch poorly. The carbon source can then be changed for faster cycling as the POI switching kinetics
650 improves during directed evolution.

651 2. Restoring *SIC1*, which makes the system less sensitive to residual Clb5, allows POIs to be
652 evolved that are initially more leaky.

653 3. Different approaches can be taken to focus directed evolution on the POI instead of the
654 optogenetic system that mediates the input to the POI, minimizing undesired solutions. One method
655 takes advantage of the statistics of mutations and uses multiple copies of the genes encoding the
656 optogenetic system in cells. This approach would have been utilized in our fifth campaign if mutations
657 in *EL222* would have overwhelmed new mutations in *PEST-rtTA*, which was not the case in our
658 experiments. The idea behind this approach is to leverage the extremely low chance that two or more
659 copies of a gene in the same cell, in our example, *EL222*, acquire mutations, much less the same type
660 of mutations (gain or loss of function). Statistically, with 'n' copies of *EL222*, activated with '1/n' fold
661 less light than for inducing cells with a single *EL222* gene, the effect of any mutation is reduced by
662 '1/n'. Even the strongest light-sensitizing mutations of El222 could thus be made ineffective for by-
663 passing selection pressure on the POI, simply by increasing the copy number of *EL222* and
664 proportionally decreasing the light duration or intensity.

665 4. A plethora of degrons can be added to reduce the activity of a POI[114].

666 5. In principle, optovolution can be extended to any POI that couples to Clb5. While we focused
667 on transcription factors here (El222, PhyB-Pif3, rtTA), Clb5 protein levels could in principle be
668 modulated by other means, including by localization and degradation. The use of more stable
669 destruction-box deficient Clb5db opens up additional such possibilities[96,115,116].

670 Further, optovolution adapts readily to POIs that function poorly initially. A general challenge with
671 directed evolution is that a POI may be so poor with respect to a desirable function that the directed
672 evolution campaign cannot even be initiated. This is mitigated in two key ways in our method: The
673 selection pressure can be easily tuned by changing the light pulse regime, e.g., shorter, longer,
674 dimmer, or brighter light pulses. In contrast, tuning of the selection pressure is not straightforward in
675 many other directed evolution methods. Furthermore, the training wheel plasmid allows proliferation
676 in the absence of any POI function, so that directed evolution of the POI can be initiated
677 concomitantly with selection for loss of the training wheel plasmid on 5-FOA.

678 In our tests, optovolution was efficient. Using the Dajbog strain, mutations in the POI gene evolved
679 efficiently and by-pass mutations were either observed rarely in Dajbog2 (*sic1Δ*) or were reasonable
680 in number to quickly find the mutation of interest with Dajbog1 (wt-*SIC1*). The system can in principle
681 be further optimized to block mutations that are not in the POI gene. After identifying such by-pass
682 mutations which lead to loss of function, one can effectively prevent them by inserting additional
683 copies of the gene. (Yeast can tolerate multiple copies of most of its genes[117,118].) Should by-pass
684 mutations occur in non-essential genes, one can in principle prevent them by deleting the gene in
685 case of gain-of-function mutations. The deep literature on cell cycle control can be leveraged for
686 improving optovolution further. Note that by-pass mutations in Cdk1 can be practically ruled out since
687 at least five mutations are required to run the cell cycle oscillator in a *cln1-3Δ clb5,6Δ* background.[90] It
688 is unknown whether quintuply mutated Cdk1 could run the Dajbog strains, which have additional
689 deletions of *CLB3,4*.

690 Another possible adaptation is to leverage the orthogonal advances that have been made to increase
691 mutation rates specifically for genes of interest. These are especially needed when mutations
692 elsewhere in the genome can readily bypass the desired POI functionality. However, Dajbog2 was
693 genetically tight, so it was not necessary to focus mutation rates on the POI gene to achieve our goals
694 here. Furthermore, our directed evolution campaigns succeeded with 1-2 mutations, obviating or
695 reducing the need to disentangle driver from passenger mutations. Using *pol3-L523D*, we expected to
696 increase the genome-wide mutation rate to $0.5 \times 10^{-7}$ per base-pair per generation[92]. This means that
697 in tens of milliliters of log-phase yeast population, about all single mutants of the POI gene should
698 have been present. Straightforward ways to increase the mutation rates further globally involve the
699 use of DNA damaging radiation and chemicals, although not all nucleotide mutations can be attained
700 in this manner. Another common method to achieve very high rates of focused mutations is to
701 introduce the POI on mutagenized plasmid libraries. Nevertheless, our method is compatible with and
702 will benefit from combining with targeted *in vivo* mutagenesis systems such as OrthoRep[15],
703 MutaT7[17,119], or CRISPR-Cas9-[120] or transposon-mediated systems[14].

704 Optovolution is particularly timely for the revolution that is currently taking place in artificial
705 intelligence-based protein design. There is a substantial interest in proteins with dynamic, multi-state,
706 and computational properties[19,121–123]. Prototypes that have been computationally designed can be
707 screened and improved in a high-throughput manner with optovolution. There is no similarly germane
708 method available for these protein functionalities currently. Additionally, machine-learning guided
709 methods will keep relying on experimentally validated training sets, which can be further enriched
710 through directed evolution. We expect optovolution to provide solutions to previously intractable
711 engineering problems and pave the way for more sophisticated proteins.

712

713 # Methods

714 ## Media

715 We used synthetic complete media[124] (SCD) with methionine (+Met) or without methionine (-Met)
716 and supplemented with 2% (w/v) glucose. For preparing solid SC plates, we used 2% agar. For
717 experiments with 5-FOA, we used a standard recipe with 0.1% 5-FOA[38,125]. For controlling and
718 evolving the transcriptionally and doxycycline-regulated AND gate (PEST-rtTA), we used 30 µM
719 doxycycline diluted from a 1000x stock in water (Sigma, USA). For characterization of the PEST-rtTA
720 variants, we used 10 µM doxycycline. For experiments with PhyB-Pif3, we used 10 µM PCB, diluted
721 from a 1000x DMSO stock (Sychem, Germany) when supplying exogenous PCB.

722 ## Plasmid construction

723 Cloning was performed using restriction enzyme digestion and ligation with T4 ligase (New England
724 Biolabs) or Gibson assembly (New England Biolabs). Plasmids were propagated in DH5alpha *E. coli* in
725 LB medium supplemented with ampicillin. See Supplementary Table 1 for a list of the plasmids.

726 ## Strain construction and preparation for directed evolution

727 Transformations of budding yeast were performed using the high-efficiency LiAc/DNA carrier/PEG
728 (polyethylene glycol) protocol[126]. All strains are derivatives of W303 (*leu2-3,112 trp1-1 can1-100 ura3-*
729 *1 ade2-1 his3-11,15*). A list of strains is provided in Supplementary Table 2.

730 The Dajbog1 (*cln1-3Δ clb3-6Δ*) and Dajbog2 (*cln1-3Δ clb3-6Δ sic1Δ*) strains proliferated in the absence
731 of light pulses in SCD-Met medium plates due to the presence of the *URA3*-marked training wheel
732 plasmid pRD-TW1 (*MET3pr-CLN2, CLB5pr-CLB5, CEN/ARS*), which was built using pRS416[127]. (Lack of
733 methionine induces *MET3pr-CLN2*.) For the different directed evolution campaigns, we built
734 additional strains starting with the Dajbog strains. To evolve *EL222* (first three campaigns), we
735 transformed the strains with *LIP-CLB5*, *LIP-CLN2*, and *PGK1pr-EL222* constructs. For the evolution of
736 the PhyB-Pif3 system (fourth campaign), we transformed them with *ADH1pr-PHYB-GALBD*, *ADH1pr-*
737 *GAL4AD-PIF3*, *GAL1pr-CLN2*, and *GAL1pr-CLB5* constructs. Lastly, for evolving the AND gate (fifth
738 campaign), we transformed the strains with *PGK1pr-EL222*, *LIP-PEST-rtTA*, *tetOpr-CLN2*, and *tetOpr-*
739 *CLB5*. We confirmed transformations by PCR.

740 To prepare the strains for directed evolution experiments, we selected for the loss of the training
741 wheel plasmid as follows: First, cells were spread on fresh SCD+Met plates and placed under pulsing
742 light. Methionine shuts off *MET3pr*, reducing any advantage that the training wheel may confer and
743 thus increasing the fraction of cells that lose the training wheel plasmid. Then, we transferred cells to

744 SCD+Met+5-FOA plates under the same pulsing light regime, so only cells that had lost the training
745 wheel plasmid could proliferate. We picked isolated colonies in which we confirmed the loss of the
746 training wheel plasmid by the lack of growth in darkness on plates lacking methionine. From then on,
747 the strains were propagated under pulsing light.

748 After directed evolution, we characterized the evolved POIs by cloning the mutated POI genes into a
749 backbone for single-copy integration. A W303 strain was transformed with these plasmids as well as
750 plasmids for single-copy integration of constructs in which the transcription of a fluorescent protein
751 was driven by *LIP* (in case of El222) or *tetOpr* (PEST-rtTA). Integration of single copies was confirmed
752 by PCR in all transformants. For measuring the transcriptional rate of PhyB-Pif3 as a split Gal4 system,
753 we used the strain from ref.[76]

## 754 Light conditions

755 Throughout, we handled cells sensitive to blue light under red light and red-responsive cells as well as
756 PCB under green light. Plates were otherwise always wrapped in aluminum foil.

757 For administering blue light to induce El222, we used commercial blue light LED panels (HQRP, USA).
758 The panels were placed inside incubators at a distance of 20 cm above the agar plates or a spinning
759 wheel of liquid cell culture tubes. For evolving color-shifted El222 variants, we used LEDs with peaks
760 around green (525 nm), yellow (575 nm), orange (615 nm), and red (660 nm) (Mouser, Switzerland).
761 For characterizing color-shifted El222 variants, we used 488 nm (JDSU, China), 514 nm (Oxxius,
762 France), 561 nm (CrystaLaser, USA), and 641 nm (Coherent, USA) lasers. For inducing optogenetics
763 during microscopy, we used diascopic light and placed a green interference filter in the optical path
764 (Nikon, Switzerland) when needed. For administering red and far-red light that switches PhyB-Pif3, we
765 used red light panels (Amats, China) with a peak around 650 nm and custom-made printed circuit
766 boards with 750 nm far-red LEDs (Roithner Lasertechnik, Austria).

767 The spectral characteristics of the light sources, measured using an ST-VIS-25 spectrometer (Ocean
768 Insight, USA) are shown in Supplementary Fig. 1.

769 To control the LEDs or lasers, we used an NI USB 6501 (Texas Instruments, USA) I/O device. The
770 system was run using a custom Matlab script (**Code availability**). The regime of pulsing light could be
771 adjusted with a precision of less than one second.

## 772 Quantification of the transition from *cln1-3Δ* arrest with optogenetic cell-cycle
## 773 control

774 To score the portion of cells that bud in response to a pulse of light (Fig. 2 B), we tested *cln1-3Δ*
775 *MET3pr-CLN2* and *cln1-3Δ clb3-6Δ pRD-TW1* cells with additional *EL222* and LIP-controlled Cdk1

776 cyclins, as indicated. After loading cells into a microfluidic chip and growing them for 4-5 hrs, we
777 supplied methionine, which shuts off *MET3pr*. Two hours after methionine had been added, cells
778 were large and unbudded (G1 arrest). Different optogenetic constructs (*LIP-CLB5* and *LIP-CLN2*) were
779 activated by using diascopic light from the microscope set to 80% of maximal intensity for 20 min or
780 40 min, depending on the experiment. Cells were imaged every 10 min.

## 781 Optovolution experiments on agar plates

782 Prior to evolution, cells were propagated under the light pulsing regime that allowed proliferation on
783 SCD agar plates until growth saturation. To increase the mutational diversity of the population, cells
784 were then mutagenized by exposing them for 10 sec to UV light with 254 nm emission peak (model
785 G30T8, Sankyo Denki, Japan). We scraped cells from one plate and resuspended them in 1 mL of liquid
786 SCD medium prewarmed to 30°C. Then, we plated 100-200 µL of cell culture on fresh agar plates and
787 chose the desired selection pressure by adjusting the light pulse regime. After three days of growth,
788 we replica-plated the cells to provide fresh nutrients. After another two days of growth, we picked
789 isolated colonies by restreaking them on fresh SCD plates, and allowed them to grow for another two
790 days. Finally, we identified the mutations by Sanger sequencing the POI gene. The whole process took
791 about seven days per screen.

## 792 Long-term continuous optovolution in liquid medium

793 As in the agar plate experiments, cells were propagated on SCD plates and UV-mutagenized. We
794 scraped cells from one plate and resuspended them in 1 mL of liquid SCD medium. We added 200 µL
795 from this suspension to 100 mL of liquid SCD medium. We used transparent 250 mL Erlenmeyer flasks
796 (VWR, Switzerland). Cell cultures were grown in an incubator shaker (Infors HT, Switzerland) set at
797 250 rotations per minute and 30°C. For administering pulsing light, we used panels of blue LEDs
798 mounted on a custom rack inside the incubator.

799 To prevent the cultures from reaching saturation, we diluted them in warm SCD medium to a final OD
800 (660 nm) of 0.04 every 12 hrs. We performed the experiment for a week, after which we proceeded
801 to Sanger sequencing bulk culture genomic DNA for the POI gene.

## 802 Mutation identification

803 To screen for mutations in the genes of interest, we performed Sanger sequencing (Microsynth AG,
804 Switzerland) using primers that span the coding sequence of interest. The identified mutations were
805 confirmed by sequencing the plasmids after cloning the POI gene.

806 For identifying mutations in the genome, we performed paired-end whole genome sequencing of the
807 evolved and ancestral genomes. The sequencing was performed using 150 bp long reads on the

808 DNBseq platform with a total data output of 1 Gb. The ancestral and the evolved reads were then
809 mapped onto the W303 reference genome using Bowtie 2. For variant calling, we used BCFtools. The
810 mutations were called if they appeared in the evolved but not the ancestral genome, and if they were
811 sequenced with a depth of at least 10.

## 812 Variant characterization

813 In all cases, strains were grown to saturation for 18-20 h, diluted, and then allowed to reach log
814 phase. Transcriptional activities were scaled to the maxGAL1 unit, where 1 maxGAL1 corresponds to
815 the steady-state expression of *GAL1pr* in synthetic complete medium containing 3% raffinose (w/v)
816 and 2% galactose (w/v)[55].

817 For characterizing the light-sensitized and color-shifted El222 variants, we cloned mutant *EL222* into
818 plasmids that inserted as single copies into the budding yeast genome, and transformed a strain that
819 contained a single-copy *LIP-ymScarletI* reporter with the plasmids. While *LIP-ymScarletI* was the
820 reporter of choice for characterizing light-sensitized variants to avoid excitation light inducing the
821 mutant El222, it has a comparatively lower sensitivity than a *yEVenus* reporter. Hence, for carefully
822 characterizing the leakiness of wt-El222 and low-leakiness variants, we introduced them into a strain
823 containing a single-copy *LIP-yEVenus* reporter. All variants were induced in log phase in liquid culture
824 for 6 h. The light-sensitized or low-leakiness variants were tested under two different light pulse
825 regimes, high or low time-averaged LED intensity (Fig. 4 B, F, J). The low LED regime corresponds to
826 the blue LEDs (Supplementary Fig. 1) pulsed for 10 sec every 5 min. The high LED regime corresponds
827 to 30 sec on, 30 sec off every minute. The color-shifted variants were induced under the presence of
828 laser light of different wavelengths (Supplementary Fig. 1). For characterizing the dynamics of the
829 evolved variants with timelapse fluorescence microscopy, we used variants of the reporters in which
830 the corresponding fluorescent proteins are fused to the PEST degron, reducing the half-life of the
831 reporters. From the measured fluorescence values we subtracted the fluorescence levels of cells
832 containing only the corresponding *LIP*-based reporter, which showed elevated fluorescence levels
833 compared to wild-type (no-reporter) cells (Supplementary Fig. 2).

834 For characterizing the effect of *yor1Δ* in combination with the PhyB-Pif3 system, we used a strain
835 from ref. [76] with a *GAL1pr-Venus* reporter. In case PCB was used, cells were incubated with it in
836 darkness for 1 hr before exposure to red light. We used 30 sec on, 30 sec off red light with an
837 emission peak around 650 nm delivered for 6 h to cells grown in SCD liquid medium tubes on a
838 spinning wheel. After that, the level of expression was measured using fluorescence microscopy.
839 Previous measurements of *GAL1pr* activity in glucose showed that it does not exhibit leakiness that is
840 distinguishable from wild-type cells without a reporter[55]. Hence, from the measured values, we
841 subtracted the background fluorescence of a wild-type strain. To convert the expression levels to

842 maxGAL1 units, we measured the steady-state expression level of *GAL1pr-Venus* in the same strain by
843 growing it in SC medium with 3% raffinose (w/v) and 2% galactose medium (w/v).

844 For quantifying the activity of PEST-rtTA mutants, we introduced them into strains with a *tetOpr-*
845 *yEVenus-PEST* reporter. We grew the strains with or without doxycycline for 6 hrs and then imaged
846 them by fluorescence microscopy. From the measured values, we subtracted the corresponding
847 background fluorescence values of the strain containing only a *tetOpr-yEVenus-PEST* reporter in the
848 corresponding medium.

### 849 Microscopy and image analysis

850 Images were recorded using a Nikon Ti2-E (Nikon, Switzerland) microscope equipped with a 60x oil,
851 N.A. 1.40 objective and a Hamamatsu Orca-Flash 4.0 camera (Hamamatsu, Japan). The microscope
852 was controlled using NIS-Elements software and the Nikon Perfect Focus System. When performing
853 timelapse microscopy to monitor the dynamic properties of EI222, we induced with diascopic light, as
854 described previously. To not induce EI222 while observing cells under the microscope, we used a
855 band-pass green interference filter (Nikon, Switzerland) placed between the diascopic light and the
856 sample. The characteristics of this light are presented in Supplementary Fig. 1. The diascopic light was
857 set to either 80% of maximal intensity, when inducing low-leakiness variants (Fig. 4 G), to 20% of
858 maximal intensity when inducing light-sensitized variants (Fig. 4 C), or to 80% of maximal intensity
859 with a green interference filter when inducing color-shifted variants (Fig. 4 K). Image analysis was
860 performed using YeaZ[98], a deep neural network for analyzing images of yeast cells.

## 861 Statistics and reproducibility

862 No statistical method was used to predetermine sample size. The values in the heatmaps in Figs. 4
863 and 7 are rounded based on the first significant digit of the standard error of the mean.

## 864 Data and material availability

865 The characteristics of the systems measured in this study have been added to the Inducible
866 Transcriptional Systems Database (https://promoter-benchmark.epfl.ch/)[55]. Any additional data that
867 support the findings of this study are available from the corresponding author upon request.

## 868 Code availability

869 The Matlab code for controlling the light pulses is available at:

870 https://github.com/rahi-lab/optogenetic_controller_script/.

871 # References


872 1. Mills, D. R., Peterson, R. L. & Spiegelman, S. An extracellular Darwinian experiment with a self-
873 duplicating nucleic acid molecule. *Proc. Natl. Acad. Sci. U.S.A.* **58**, 217–224 (1967).
874 2. Kuchner, O. & Arnold, F. H. Directed evolution of enzyme catalysts. *Trends in Biotechnology* **15**,
875 523–530 (1997).
876 3. Schmidt-Dannert, C. & Arnold, F. H. Directed evolution of industrial enzymes. *Trends in*
877 *Biotechnology* **17**, 135–136 (1999).
878 4. Packer, M. S. & Liu, D. R. Methods for the directed evolution of proteins. *Nat Rev Genet* **16**, 379–
879 394 (2015).
880 5. Wang, Y. *et al.* Directed Evolution: Methodologies and Applications. *Chem. Rev.* **121**, 12384–
881 12444 (2021).
882 6. Crameri, A., Whitehorn, E. A., Tate, E. & Stemmer, W. P. C. Improved Green Fluorescent Protein
883 by Molecular Evolution Using DNA Shuffling. *Nat Biotechnol* **14**, 315–319 (1996).
884 7. Campbell, R. E. *et al.* A monomeric red fluorescent protein. *Proc. Natl. Acad. Sci. U.S.A.* **99**, 7877–
885 7882 (2002).
886 8. Li, Y. *et al.* Directed evolution of human T-cell receptors with picomolar affinities by phage display.
887 *Nat Biotechnol* **23**, 349–354 (2005).
888 9. Xu, L. *et al.* Directed Evolution of High-Affinity Antibody Mimics Using mRNA Display. *Chemistry &*
889 *Biology* **9**, 933–942 (2002).
890 10. Arnold, F. H. Design by Directed Evolution. *Acc. Chem. Res.* **31**, 125–131 (1998).
891 11. Esvelt, K. M., Carlson, J. C. & Liu, D. R. A system for the continuous directed evolution of
892 biomolecules. *Nature* **472**, 499–503 (2011).

893 12. Badran, A. H. & Liu, D. R. In vivo continuous directed evolution. *Current Opinion in Chemical*
894 *Biology* **24**, 1–10 (2015).
895 13. Molina, R. S. *et al.* In vivo hypermutation and continuous evolution. *Nat Rev Methods Primers* **2**,
896 36 (2022).
897 14. Crook, N. *et al.* In vivo continuous evolution of genes and pathways in yeast. *Nat Commun* **7**,
898 13051 (2016).
899 15. Ravikumar, A., Arzumanyan, G. A., Obadi, M. K. A., Javanpour, A. A. & Liu, C. C. Scalable,
900 Continuous Evolution of Genes at Mutation Rates above Genomic Error Thresholds. *Cell* **175**,
901 1946-1957.e13 (2018).
902 16. Yi, X., Khey, J., Kazlauskas, R. J. & Travisano, M. Plasmid hypermutation using a targeted artificial
903 DNA replisome. *Sci. Adv.* **7**, eabg8712 (2021).
904 17. Moore, C. L., Papa, L. J. & Shoulders, M. D. A Processive Protein Chimera Introduces Mutations
905 across Defined DNA Regions *In Vivo*. *J. Am. Chem. Soc.* **140**, 11560–11564 (2018).
906 18. Sadeghi, A., Dervey, R., Gligorovski, V., Labagnara, M. & Rahi, S. J. The optimal strategy balancing
907 risk and speed predicts DNA damage checkpoint override times. *Nat. Phys.* (2022)
908 doi:10.1038/s41567-022-01601-3.
909 19. Chen, Z. *et al.* De novo design of protein logic gates. *Science* **368**, 78–84 (2020).
910 20. Gao, X. J., Chong, L. S., Kim, M. S. & Elowitz, M. B. Programmable protein circuits in living cells.
911 *Science* **361**, 1252–1258 (2018).
912 21. Fink, T. *et al.* Design of fast proteolysis-based signaling and logic circuits in mammalian cells. *Nat*
913 *Chem Biol* **15**, 115–122 (2019).
914 22. Omersa, N., Aden, S., Kisovec, M., Podobnik, M. & Anderluh, G. Design of Protein Logic Gate
915 System Operating on Lipid Membranes. *ACS Synth. Biol.* **9**, 316–328 (2020).

916 23. Vishweshwaraiah, Y. L., Chen, J., Chirasani, V. R., Tabdanov, E. D. & Dokholyan, N. V. Two-input
917 protein logic gate for computation in living cells. *Nat Commun* **12**, 6615 (2021).
918 24. Berman, C. M. *et al.* An Adaptable Platform for Directed Evolution in Human Cells. *J. Am. Chem.*
919 *Soc.* **140**, 18093–18103 (2018).
920 25. English, J. G. *et al.* VEGAS as a Platform for Facile Directed Evolution in Mammalian Cells. *Cell* **178**,
921 748-761.e17 (2019).
922 26. Woloschuk, R. M., Reed, P. M. M., McDonald, S., Uppalapati, M. & Woolley, G. A. Yeast Two-
923 Hybrid Screening of Photoswitchable Protein–Protein Interaction Libraries. *Journal of Molecular*
924 *Biology* **432**, 3113–3126 (2020).
925 27. Taslimi, A. *et al.* Optimized second-generation CRY2–CIB dimerizers and photoactivatable Cre
926 recombinase. *Nat Chem Biol* **12**, 425–430 (2016).
927 28. Kawano, F., Aono, Y., Suzuki, H. & Sato, M. Fluorescence Imaging-Based High-Throughput
928 Screening of Fast- and Slow-Cycling LOV Proteins. *PLoS ONE* **8**, e82693 (2013).
929 29. Wang, W. *et al.* A light- and calcium-gated transcription factor for imaging and manipulating
930 activated neurons. *Nat Biotechnol* **35**, 864–871 (2017).
931 30. Sanchez, M. I. & Ting, A. Y. Directed evolution improves the catalytic efficiency of TEV protease.
932 *Nat Methods* **17**, 167–174 (2020).
933 31. Ryu, M.-H. *et al.* Engineering adenylate cyclases regulated by near-infrared window light. *Proc.*
934 *Natl. Acad. Sci. U.S.A.* **111**, 10167–10172 (2014).
935 32. Richter, F. *et al.* Engineering of temperature- and light-switchable Cas9 variants. *Nucleic Acids*
936 *Research* **44**, gkw930 (2013).

937 33. Kaberniuk, A. A., Baloban, M., Monakhov, M. V., Shcherbakova, D. M. & Verkhusha, V. V. Single-
938 component near-infrared optogenetic systems for gene transcription regulation. *Nat Commun* **12**,
939 3859 (2021).
940 34. Baumschlager, A., Weber, Y., Cánovas, D., Dionisi, S. & Khammash, M. *Enhancing the Performance*
941 *of Magnets Photosensors through Directed Evolution*.
942 http://biorxiv.org/lookup/doi/10.1101/2022.11.14.516313 (2022)
943 doi:10.1101/2022.11.14.516313.
944 35. Reis, J. M. *et al.* Discovering Selective Binders for Photoswitchable Proteins Using Phage Display.
945 *ACS Synth. Biol.* **7**, 2355–2364 (2018).
946 36. Wang, H. *et al.* LOVTRAP: an optogenetic system for photoinduced protein dissociation. *Nat*
947 *Methods* **13**, 755–758 (2016).
948 37. Guntas, G. *et al.* Engineering an improved light-induced dimer (iLID) for controlling the localization
949 and activity of signaling proteins. *Proc. Natl. Acad. Sci. U.S.A.* **112**, 112–117 (2015).
950 38. Boeke, J. D., Trueheart, J., Natsoulis, G. & Fink, G. R. [10] 5-Fluoroorotic acid as a selective agent in
951 yeast molecular genetics. in *Methods in Enzymology* vol. 154 164–175 (Elsevier, 1987).
952 39. Tague, N., Coriano-Ortiz, C., Sheets, M. B. & Dunlop, M. J. *Light Inducible Protein Degradation in E.*
953 *Coli with the LOVdeg Tag*. https://elifesciences.org/reviewed-preprints/87303v2 (2024)
954 doi:10.7554/eLife.87303.2.
955 40. Nguyen, N. T., Liu, S., Han, G., Zhou, Y. & Huang, K. Nano-optogenetic CAR-T Cell Immunotherapy.
956 in *Cancer Immunotherapy* (eds. Siciliano, V. & Ceroni, F.) vol. 2748 267–278 (Springer US, New
957 York, NY, 2024).

958 41. Song, G. *et al.* Rapid characterization of anti-CRISPR proteins and optogenetically engineered
959 variants using a versatile plasmid interference system. *Nucleic Acids Research* **51**, 12381–12396
960 (2023).
961 42. Levskaya, A., Weiner, O. D., Lim, W. A. & Voigt, C. A. Spatiotemporal control of cell signalling using
962 a light-switchable protein interaction. *Nature* **461**, 997–1001 (2009).
963 43. Cui, M. *et al.* A single-component, light-assisted uncaging switch for endoproteolytic release. *Nat*
964 *Chem Biol* (2023) doi:10.1038/s41589-023-01480-6.
965 44. Nzigou Mombo, B. *et al.* Reversible photoregulation of cell-cell adhesions with opto-E-cadherin.
966 *Nat Commun* **14**, 6292 (2023).
967 45. Legnini, I. *et al.* Spatiotemporal, optogenetic control of gene expression in organoids. *Nat*
968 *Methods* **20**, 1544–1552 (2023).
969 46. Ho, E. K. *et al.* Dynamics of an incoherent feedforward loop drive ERK-dependent pattern
970 formation in the early *Drosophila* embryo. *Development* **150**, dev201818 (2023).
971 47. Pal, A. A. *et al.* Optogenetic clustering and membrane translocation of the BcLOV4 photoreceptor.
972 *Proc. Natl. Acad. Sci. U.S.A.* **120**, e2221615120 (2023).
973 48. Mahlandt, E. K. *et al.* Opto-RhoGEFs, an optimized optogenetic toolbox to reversibly control Rho
974 GTPase activity on a global to subcellular scale, enabling precise control over vascular endothelial
975 barrier strength. *eLife* **12**, RP84364 (2023).
976 49. Lim, C. K., Yeoh, J. W., Kunartama, A. A., Yew, W. S. & Poh, C. L. A biological camera that captures
977 and stores images directly into DNA. *Nat Commun* **14**, 3921 (2023).
978 50. Elsaid, R., Mikdache, A., Diabangouaya, P., Gros, G. & Hernández, P. P. *A Non-Invasive*
979 *Photoactivatable Split-Cre Recombinase System for Genome Engineering in Zebrafish*.

980 http://biorxiv.org/lookup/doi/10.1101/2023.06.23.546268 (2023)
981 doi:10.1101/2023.06.23.546268.
982 51. De Belly, H. *et al.* Cell protrusions and contractions generate long-range membrane tension
983 propagation. *Cell* **186**, 3049-3061.e15 (2023).
984 52. Benisch, M., Benzinger, D., Kumar, S., Hu, H. & Khammash, M. Optogenetic closed-loop feedback
985 control of the unfolded protein response optimizes protein production. *Metabolic Engineering* **77**,
986 32–40 (2023).
987 53. Sheets, M. B., Tague, N. & Dunlop, M. J. An optogenetic toolkit for light-inducible antibiotic
988 resistance. *Nat Commun* **14**, 1034 (2023).
989 54. Zoltowski, B. D., Vaccaro, B. & Crane, B. R. Mechanism-based tuning of a LOV domain
990 photoreceptor. *Nat Chem Biol* **5**, 827–834 (2009).
991 55. Gligorovski, V., Sadeghi, A. & Rahi, S. J. Multidimensional characterization of inducible promoters
992 and a highly light-sensitive LOV-transcription factor. *Nat Commun* **14**, 3810 (2023).
993 56. Pudasaini, A., El-Arab, K. K. & Zoltowski, B. D. LOV-based optogenetic devices: light-driven
994 modules to impart photoregulated control of cellular signaling. *Front. Mol. Biosci.* **2**, (2015).
995 57. Adir, O. *et al.* Synthetic cells with self-activating optogenetic proteins communicate with natural
996 cells. *Nat Commun* **13**, 2328 (2022).
997 58. Pan, H. *et al.* Engineered NIR light-responsive bacteria as anti-tumor agent for targeted and
998 precise cancer therapy. *Chemical Engineering Journal* **426**, 130842 (2021).
999 59. Wang, Z., Yan, Y. & Zhang, H. Design and Characterization of an Optogenetic System in *Pichia*
1000 *pastoris*. *ACS Synth. Biol.* **11**, 297–307 (2022).
1001 60. Zhao, E. M. *et al.* Optogenetic regulation of engineered cellular metabolism for microbial chemical
1002 production. *Nature* **555**, 683–687 (2018).

1003 61. Motta-Mena, L. B. *et al.* An optogenetic gene expression system with rapid activation and
1004 deactivation kinetics. *Nat Chem Biol* **10**, 196–202 (2014).
1005 62. Baaske, J. *et al.* Dual-controlled optogenetic system for the rapid down-regulation of protein
1006 levels in mammalian cells. *Sci Rep* **8**, 15024 (2018).
1007 63. LaBelle, J. *et al.* TAEL 2.0: An Improved Optogenetic Expression System for Zebrafish. *Zebrafish* **18**,
1008 20–28 (2021).
1009 64. Molin, M. *et al.* Protein kinase A controls yeast growth in visible light. *BMC Biol* **18**, 168 (2020).
1010 65. Barolet, D. Light-Emitting Diodes (LEDs) in Dermatology. *Seminars in Cutaneous Medicine and*
1011 *Surgery* **27**, 227–238 (2008).
1012 66. Akagi, H., Shimizu, H. & Toya, Y. Multicolor optogenetics for regulating flux ratio of three glycolytic
1013 pathways using EL222 and CcaSR in *Escherichia coli*. *Biotech & Bioengineering* bit.28628 (2023)
1014 doi:10.1002/bit.28628.
1015 67. Kramer, M. M., Mühlhäuser, W. W. D., Weber, W. & Radziwill, G. Multichromatic Control of
1016 Signaling Pathways in Mammalian Cells. *Advanced Biology* **5**, 2000196 (2021).
1017 68. Ochoa-Fernandez, R. *et al.* Optogenetic control of gene expression in plants in the presence of
1018 ambient white light. *Nat Methods* **17**, 717–725 (2020).
1019 69. Redchuk, T. A. *et al.* Optogenetic regulation of endogenous proteins. *Nat Commun* **11**, 605 (2020).
1020 70. Losi, A., Gardner, K. H. & Möglich, A. Blue-Light Receptors for Optogenetics. *Chem. Rev.* **118**,
1021 10659–10709 (2018).
1022 71. Remeeva, A. *et al.* Insights into the mechanisms of light-oxygen-voltage domain color tuning from
1023 a set of high-resolution X-ray structures. *Proteins* **89**, 1005–1016 (2021).
1024 72. Toettcher, J. E., Gong, D., Lim, W. A. & Weiner, O. D. Light-based feedback for controlling
1025 intracellular signaling dynamics. *Nat Methods* **8**, 837–839 (2011).

1026 73. Yang, X., Jost, A. P.-T., Weiner, O. D. & Tang, C. A light-inducible organelle-targeting system for
1027 dynamically activating and inactivating signaling in budding yeast. *MBoC* **24**, 2419–2430 (2013).
1028 74. Shimizu-Sato, S., Huq, E., Tepperman, J. M. & Quail, P. H. A light-switchable gene promoter
1029 system. *Nat Biotechnol* **20**, 1041–1044 (2002).
1030 75. Pathak, G. P., Strickland, D., Vrana, J. D. & Tucker, C. L. Benchmarking of optical dimerizer systems.
1031 *ACS Synth. Biol.* **3**, 832–838 (2014).
1032 76. Milias-Argeitis, A. *et al. In silico* feedback for in vivo regulation of a gene expression circuit. *Nat*
1033 *Biotechnol* **29**, 1114–1116 (2011).
1034 77. Oda, S., Sato-Ebine, E., Nakamura, A., Kimura, K. D. & Aoki, K. *Optogenetic Control of Cell Signaling*
1035 *with Red/Far-Red Light-Responsive Optogenetic Tools in* Caenorhabditis Elegans.
1036 http://biorxiv.org/lookup/doi/10.1101/2022.08.12.503710 (2022)
1037 doi:10.1101/2022.08.12.503710.
1038 78. Uda, Y. *et al.* Efficient synthesis of phycocyanobilin in mammalian cells for optogenetic control of
1039 cell signaling. *Proc. Natl. Acad. Sci. U.S.A.* **114**, 11962–11967 (2017).
1040 79. Müller, K. *et al.* Synthesis of phycocyanobilin in mammalian cells. *Chem. Commun.* **49**, 8970
1041 (2013).
1042 80. Hochrein, L., Machens, F., Messerschmidt, K. & Mueller-Roeber, B. PhiReX: a programmable and
1043 red light-regulated protein expression switch for yeast. *Nucleic Acids Research* **45**, 9193–9205
1044 (2017).
1045 81. Gossen, M. *et al.* Transcriptional Activation by Tetracyclines in Mammalian Cells. *Science* **268**,
1046 1766–1769 (1995).
1047 82. Mateus, C. & Avery, S. V. Destabilized green fluorescent protein for monitoring dynamic changes
1048 in yeast gene expression with flow cytometry. *Yeast* **16**, 1313–1323 (2000).

1049 83. Rahi, S. J., Pecani, K., Ondracka, A., Oikonomou, C. & Cross, F. R. The CDK-APC/C oscillator
1050 predominantly entrains periodic cell-cycle transcription. *Cell* **165**, 475–487 (2016).
1051 84. Richardson, H., Lew, D. J., Henze, M., Sugimoto, K. & Reed, S. I. Cyclin-B homologs in
1052 Saccharomyces cerevisiae function in S phase and in G2. *Genes Dev.* **6**, 2021–2034 (1992).
1053 85. Cross, F. R., Schroeder, L., Kruse, M. & Chen, K. C. Quantitative Characterization of a Mitotic Cyclin
1054 Threshold Regulating Exit from Mitosis. *MBoC* **16**, 2129–2138 (2005).
1055 86. Surana, U. *et al.* Destruction of the CDC28/CLB mitotic kinase is not required for the metaphase to
1056 anaphase transition in budding yeast. *The EMBO Journal* **12**, 1969–1978 (1993).
1057 87. Rahi, S. J. *et al.* Oscillatory stimuli differentiate adapting circuit topologies. *Nat Methods* **14**, 1010–
1058 1016 (2017).
1059 88. Loog, M. & Morgan, D. O. Cyclin specificity in the phosphorylation of cyclin-dependent kinase
1060 substrates. *Nature* **434**, 104–108 (2005).
1061 89. Morgan, D. O. *The Cell Cycle: Principles of Control*. (Published by New Science Press in association
1062 with Oxford University Press; Distributed inside North America by Sinauer Associates, Publishers,
1063 London: Sunderland, MA, 2007).
1064 90. Cross, F. R. & Levine, K. Molecular Evolution Allows Bypass of the Requirement for Activation Loop
1065 Phosphorylation of the Cdc28 Cyclin-Dependent Kinase. *Molecular and Cellular Biology* **18**, 2923–
1066 2931 (1998).
1067 91. Tyers, M. The cyclin-dependent kinase inhibitor p40SIC1 imposes the requirement for Cln G1
1068 cyclin function at Start. *Proc. Natl. Acad. Sci. U.S.A.* **93**, 7772–7776 (1996).
1069 92. Jin, Y. H. *et al.* The Multiple Biological Roles of the 3→5 Exonuclease of *Saccharomyces*
1070 *cerevisiae* DNA Polymerase δ Require Switching between the Polymerase and Exonuclease
1071 Domains. *Molecular and Cellular Biology* **25**, 461–471 (2005).

1072 93. Lang, G. I. & Murray, A. W. Estimating the Per-Base-Pair Mutation Rate in the Yeast
1073 *Saccharomyces cerevisiae*. *Genetics* **178**, 67–82 (2008).
1074 94. Dahmann, C., Diffley, J. F. X. & Nasmyth, K. A. S-phase-promoting cyclin-dependent kinases
1075 prevent re-replication by inhibiting the transition of replication origins to a pre-replicative state.
1076 *Current Biology* **5**, 1257–1269 (1995).
1077 95. Nguyen, V. Q., Co, C. & Li, J. J. Cyclin-dependent kinases prevent DNA re-replication through
1078 multiple mechanisms. *Nature* **411**, 1068–1073 (2001).
1079 96. Jacobson, M. D., Gray, S., Yuste-Rojas, M. & Cross, F. R. Testing cyclin specificity in the exit from
1080 mitosis. *Mol Cell Biol* **20**, 4483–4493 (2000).
1081 97. Kozholianko, G. SOLAR CULT OF ANCIENT UKRAINIANS. *nz* **139**, 57–64 (2018).
1082 98. Dietler, N. *et al.* A convolutional neural network segments yeast microscopy images with high
1083 accuracy. *Nat Commun* **11**, 5723 (2020).
1084 99. Nash, A. I. *et al.* Structural basis of photosensitivity in a bacterial light-oxygen-voltage/helix-turn-
1085 helix (LOV-HTH) DNA-binding protein. *Proc. Natl. Acad. Sci. U.S.A.* **108**, 9449–9454 (2011).
1086 100. Zoltowski, B. D., Motta-Mena, L. B. & Gardner, K. H. Blue light-induced dimerization of a
1087 bacterial LOV–HTH DNA-binding protein. *Biochemistry* **52**, 6653–6661 (2013).
1088 101. Glantz, S. T. *et al.* Functional and topological diversity of LOV domain photoreceptors. *Proc.*
1089 *Natl. Acad. Sci. U.S.A.* **113**, (2016).
1090 102. Swartz, T. E. *et al.* The Photocycle of a Flavin-binding Domain of the Blue Light Photoreceptor
1091 Phototropin. *Journal of Biological Chemistry* **276**, 36493–36500 (2001).
1092 103. Yee, E. F. *et al.* Signal transduction in light–oxygen–voltage receptors lacking the adduct-
1093 forming cysteine residue. *Nat Commun* **6**, 10079 (2015).

1094 104. Miller, B. G. & Wolfenden, R. Catalytic Proficiency: The Unusual Case of OMP Decarboxylase.
1095 *Annu. Rev. Biochem.* **71**, 847–885 (2002).
1096 105. Cui, Z., Hirata, D., Tsuchiya, E., Osada, H. & Miyakawa, T. The Multidrug Resistance-associated
1097 Protein (MRP) Subfamily (Yrs1/Yor1) of Is Important for the Tolerance to a Broad Range of Organic
1098 Anions. *Journal of Biological Chemistry* **271**, 14712–14716 (1996).
1099 106. Szczypka, M. S., Wemmie, J. A., Moye-Rowley, W. S. & Thiele, D. J. A yeast metal resistance
1100 protein similar to human cystic fibrosis transmembrane conductance regulator (CFTR) and
1101 multidrug resistance-associated protein. *Journal of Biological Chemistry* **269**, 22853–22857 (1994).
1102 107. Allard, C. A. H., Decker, F., Weiner, O. D., Toettcher, J. E. & Graziano, B. R. A size-invariant bud-
1103 duration timer enables robustness in yeast cell size control. *PLoS ONE* **13**, e0209301 (2018).
1104 108. Zhou, X., Vink, M., Klaver, B., Berkhout, B. & Das, A. T. Optimization of the Tet-On system for
1105 regulated gene expression through viral evolution. *Gene Ther* **13**, 1382–1390 (2006).
1106 109. Alberstein, R. G., Guo, A. B. & Kortemme, T. Design principles of protein switches. *Current*
1107 *Opinion in Structural Biology* **72**, 71–78 (2022).
1108 110. Pillai, A. *et al. De Novo Design of Allosterically Switchable Protein Assemblies*.
1109 http://biorxiv.org/lookup/doi/10.1101/2023.11.01.565167 (2023)
1110 doi:10.1101/2023.11.01.565167.
1111 111. Glasgow, A. A. *et al.* Computational design of a modular protein sense-response system.
1112 *Science* **366**, 1024–1028 (2019).
1113 112. Kretschmer, S., Perry, N., Zhang, Y. & Kortemme, T. Multi-input Drug-Controlled Switches of
1114 Mammalian Gene Expression Based on Engineered Nuclear Hormone Receptors. *ACS Synth. Biol.*
1115 **12**, 1924–1934 (2023).

1116 113. Jefferson, R. E. *et al.* Computational design of dynamic receptor—peptide signaling complexes
1117 applied to chemotaxis. *Nat Commun* **14**, 2875 (2023).
1118 114. Yu, H. *et al.* Conserved Sequence Preferences Contribute to Substrate Recognition by the
1119 Proteasome. *Journal of Biological Chemistry* **291**, 14526–14539 (2016).
1120 115. Sari, F., Braus, G. H. & Irniger, S. A Process Independent of the Anaphase-promoting Complex
1121 Contributes to Instability of the Yeast S Phase Cyclin Clb5. *Journal of Biological Chemistry* **282**,
1122 26614–26622 (2007).
1123 116. Wäsch, R. & Cross, F. R. APC-dependent proteolysis of the mitotic cyclin Clb2 is essential for
1124 mitotic exit. *Nature* **418**, 556–562 (2002).
1125 117. Makanae, K., Kintaka, R., Makino, T., Kitano, H. & Moriya, H. Identification of dosage-sensitive
1126 genes in *Saccharomyces cerevisiae* using the genetic tug-of-war method. *Genome Res.* **23**, 300–
1127 311 (2013).
1128 118. Robinson, D., Place, M., Hose, J., Jochem, A. & Gasch, A. P. Natural variation in the
1129 consequences of gene overexpression and its implications for evolutionary trajectories. *eLife* **10**,
1130 e70564 (2021).
1131 119. Cravens, A., Jamil, O. K., Kong, D., Sockolosky, J. T. & Smolke, C. D. Polymerase-guided base
1132 editing enables in vivo mutagenesis and rapid protein engineering. *Nat Commun* **12**, 1579 (2021).
1133 120. Skrekas, C., Limeta, A., Siewers, V. & David, F. Targeted *In Vivo* Mutagenesis in Yeast Using
1134 CRISPR/Cas9 and Hyperactive Cytidine and Adenine Deaminases. *ACS Synth. Biol.* **12**, 2278–2289
1135 (2023).
1136 121. Ng, A. H. *et al.* Modular and tunable biological feedback control using a de novo protein
1137 switch. *Nature* **572**, 265–269 (2019).
1138 122. Langan, R. A. *et al.* De novo design of bioactive protein switches. *Nature* **572**, 205–210 (2019).

1139 123. Shui, S., Scheller, L. & Correia, B. E. *Rationally Designed Protein Bandpass Filters for Controlling*
1140 *Cellular Signaling with Chemical Inputs*.
1141 http://biorxiv.org/lookup/doi/10.1101/2023.02.10.528077 (2023)
1142 doi:10.1101/2023.02.10.528077.
1143 124. Synthetic complete (SC) medium. *Cold Spring Harb Protoc* **2016**, pdb.rec090589 (2016).
1144 125. 5-Fluoroorotic Acid (5-FOA) Plates. *Cold Spring Harb Protoc* **2016**, pdb.rec086637 (2016).
1145 126. Gietz, R. D. & Schiestl, R. H. High-efficiency yeast transformation using the LiAc/SS carrier
1146 DNA/PEG method. *Nat Protoc* **2**, 31–34 (2007).
1147 127. Sikorski, R. S. & Hieter, P. A system of shuttle vectors and yeast host strains designed for
1148 efficient manipulation of DNA in Saccharomyces cerevisiae. *Genetics* **122**, 19–27 (1989).
1149 128. Rivera-Cancel, G., Motta-Mena, L. B. & Gardner, K. H. Identification of natural and artificial
1150 DNA substrates for light-activated LOV–HTH transcription factor EL222. *Biochemistry* **51**, 10024–
1151 10034 (2012).
1152 129. Epstein, C. B. & Cross, F. R. CLB5: a novel B cyclin from budding yeast with a role in S phase.
1153 *Genes Dev.* **6**, 1695–1706 (1992).
1154 130. Orlando, D. A. *et al.* Global control of cell-cycle transcription by coupled CDK and network
1155 oscillators. *Nature* **453**, 944–947 (2008).
1156 131. Yang, X., Lau, K.-Y., Sevim, V. & Tang, C. Design Principles of the Yeast G1/S Switch. *PLoS Biol*
1157 **11**, e1001673 (2013).
1158 132. Lengronne, A. & Schwob, E. The Yeast CDK Inhibitor Sic1 Prevents Genomic Instability by
1159 Promoting Replication Origin Licensing in Late G1. *Molecular Cell* **9**, 1067–1078 (2002).
1160 133. Quail, P. H. Phytochromes. *Current Biology* **20**, R504–R507 (2010).

1161 134. Quail, P. H. *et al.* Phytochromes: Photosensory Perception and Signal Transduction. *Science*
1162 **268**, 675–680 (1995).
1163 135. Liu, C., Fu, Y., Lin, L., Elson, E. L. & Wang, J. Understanding Cellular Noise with Optical
1164 Perturbation and Deep Learning. (2024) doi:10.48550/ARXIV.2401.12498.
1165 136. Sharrock, R. A. The phytochrome red/far-red photoreceptor superfamily. *Genome Biol* **9**, 230
1166 (2008).
1167 137. Baron, U. & Bujard, H. Tet repressor-based system for regulated gene expression in eukaryotic
1168 cells: Principles and advances. in *Methods in Enzymology* vol. 327 401–421 (Elsevier, 2000).
1169
1170

1171 # Acknowledgments

1172 We thank Roxane Dervey for help with strain construction and media preparation; Dr. Kyle Douglass
1173 and Prof. Suliana Manley for help with the laser experiments; Prof. Peter Quail, Prof. Hana El-Samad,
1174 and Dr. Brian Graziano for providing PhyB-Pif3 strains and constructs; Prof. José L. Avalos and Dr. Evan
1175 Zhao for providing the *EL222* plasmid; Prof. Andrew Murray for providing the *pol3-L523D* strain; and
1176 Dr. Enrico Tenaglia for help with molecular cloning. We thank the mechanical and electronics
1177 workshops of the Institute of Physics in the Cubotron building at EPFL for help building the hardware
1178 for optogenetic stimulation. We acknowledge support for VG, ML, and SJR provided by SNSF grants
1179 CRSK-3_190526 and 310030_204938 awarded to SJR.

1180 # Author contributions

1181 VG and SJR designed the experiments and analyzed the data. VG constructed the strains used for
1182 evolution. VG performed the directed evolution experiments. VG and ML characterized the evolved
1183 variants by fluorescence microscopy. VG and SJR wrote the manuscript. SJR supervised the work and
1184 acquired funding.

1185 # Competing interests

1186 VG and SJR have filed a provisional patent application for the method reported in this manuscript
1187 through EPFL.

1188

# Supplementary Material

## Supplementary Note 1: El222 optogenetic system

El222 is a transcription factor from marine bacterium *Erythrobacter litoralis*.[100] El222 has been adapted for use in eukaryotes by way of a tandem fusion of the prokaryotic El222 transcription factor, a nuclear localization signal, and the VP16 transcriptional activation domain. In darkness, the interaction of the helix-turn-helix (HTH) DNA binding domain with DNA is sterically hindered by the light-sensing LOV-domain[99]. Upon blue light illumination, a covalent bond is formed between the Cys-75 residue and the flavin chromophore[102]. (All references to mutant residue numbers in El222 are given with respect to bacterial El222 to match the numbering used in previous work[55,99,100].) This leads to a conformational change, which dislocates the Jα helix of the LOV domain. Subsequently, the protein forms a homodimer and binds to the DNA substrate using its exposed HTH domain. In the absence of blue light, the protein reverts to its ground state. For brevity, we refer to the promoter consisting of 5 El222 binding sites[128] upstream of a minimal eukaryotic promoter as *LIP*.

1203 # Supplementary Note 2: Summary of cell cycle biology relevant to
1204 optovolution

1205 ## Wild-type cell cycle control

1206 In this note, we briefly summarize the wild-type model of cell cycle control in budding yeast.[89] In the
1207 next section, we focus on how the cell cycle runs in the Dajbog strains.

1208 At the biochemical level, the rhythm of the cell-cycle oscillator is predominantly generated by a
1209 negative feedback loop[87]. In this loop, cyclin-dependent kinase (CDK) and the anaphase-promoting
1210 complex/cyclosome (APC/C) alternate in activity and drive cell cycle progression.

1211 In budding yeast, there is a single cyclin-dependent kinase, Cdk1 (also known as Cdc28). Processes
1212 that Cdk1 controls include the transcription of hundreds of cell cycle-periodic genes, DNA replication,
1213 spindle pole body duplication, and spindle formation. Activity and specificity of Cdk1 towards
1214 different substrates is mainly regulated through its interaction with regulatory proteins called cyclins.
1215 Different cyclins generally promote distinct cell-cycle events and are expressed at different stages of
1216 the cell cycle. In *S. cerevisiae*, cyclins are commonly classified into four groups: G1, G1/S, S, and M
1217 cyclins. Each cyclin-Cdk complex promotes the activation of the next group of cyclins.

1218 The G1 cyclin Cln3 activates G1/S cyclins Cln1 and Cln2 and has a role in cell-cycle entry in response to
1219 growth. Cln1-3 are responsible for the initiation of formation of the daughter cell and expression of
1220 the 100s of genes of the Start regulon. At the onset of S phase, levels of S cyclins Clb5 and Clb6 rise.
1221 Their association with Cdk1 is primarily responsible for the initiation of DNA replication by triggering
1222 the activation of origins of replication. Approaching mitosis, the concentrations of the remaining B-
1223 type cyclins increase. In budding yeast, there are four such cyclins, Clb1, Clb2, Clb3, and Clb4. Their
1224 association with Cdk1 enables assembly of the mitotic spindle and attachment of chromosomes to the
1225 spindle.

1226 In order to enable mitotic exit and reset the state of the cell for new cell cycles, cyclins have to be
1227 inactivated. While the activity G1/S cyclins is brought down by degradation and inhibition of the
1228 transcription factor SBF, S and M phase cyclins are not degraded until anaphase. At least two different
1229 mechanisms help repress Clb cyclin activity. The first one is through the activation of APC/C by the
1230 proteins Cdc20 and Cdh1. APC/C is a ubiquitin ligase complex that marks cyclins for degradation by
1231 the proteasome. The second mechanism is through the protein Sic1, which stoichiometrically inhibits
1232 Cdk1-Clb complexes, thereby effectively reducing their activity.

1233 ## Rewired cell cycle control in the Dajbog strains

1234 Although cyclins are specialized for certain phases of the cell cycle, the functions of some cyclins
1235 overlap. For example, when overexpressed, S phase cyclin Clb5 can initiate budding in a *cln1-3Δ*
1236 block[129]. Similarly, the M-phase cyclins Clb1[130]or Clb2[83]can assume the roles of all other Clb cyclins in
1237 a *clb1-6Δ* background. Endogenous *CLB3-6* genes also suffice for cell cycle start when the Clb-cyclin
1238 inhibitor *SIC1* is deleted, rendering *cln1-3Δ sic1Δ* cells viable[91].

1239 While G1/S cyclin and S cyclin expression initiates at about the same time under the control of
1240 transcription factors Sbf and Mbf[89], respectively, S cyclins are inactive until G1/S cyclins have
1241 sufficiently degraded Sic1 and Cdh1. Thus, in wild-type cells, although *CLN2* and *CLB5* are
1242 simultaneously transcriptionally activated, there is a delay between G1/S-Cdk and S-Cdk activity[89,131].
1243 We expect this delay to persist in Dajbog1 cells. Deleting *SIC1* in Dajbog2 cells is expected to cause an
1244 increase in chromosomal rearrangements due to premature S-Cdk activity[132] but this did not
1245 noticeably interfere with our directed evolution experiments.

1246 Clb5-Cdk1 leads to the firing of origins of replication in S phase. Overexpression of destruction box
1247 deficient Clb5db in galactose medium arrests the cell cycle by inhibiting the formation of pre-
1248 replicative origins, a process known as origin of replication relicensing[94–96]. This represents the
1249 expected mechanism for the lethality of *CLB5* overexpression in glucose medium. This observation led
1250 us to further sensitize Dajbog1 cells to continuous Clb5 activity by deleting *SIC1*, resulting in Dajbog2
1251 strains.

1252

1253 # Supplementary Note 3: PhyB-Pif3 optogenetic system

1254 Phytochromes are photosensors in plants, bacteria, and fungi[133]. Phytochrome B and its interaction
1255 partner Pif3 are used by plants to adapt gene expression to environmental light conditions[134].

1256 The light-inducible PhyB-Pif3 interaction has been extensively used in organisms other than plants[72–
1257 75]. By fusing one protein to PhyB and another to Pif3, one can induce protein-protein interactions in a
1258 temporarily and spatially precise manner, for example, in order to sequester proteins to specific
1259 cellular compartments[73]. In the yeast two-hybrid version of the system, it is used for light-inducible
1260 transcriptional control in budding yeast.[74,135] Typically, PhyB and Pif3 are fused to the Gal4 DNA
1261 binding domain and the Gal4 transcriptional activation domain, respectively.[74] When bound to its
1262 chromophore and activated by red light (≈650 nm), PhyB binds Pif3, thereby, bringing the
1263 transcriptional activation and DNA binding domains close together, which leads to the expression of
1264 the *GAL* family of genes. In the presence of far-red light (≈ 740 nm) or prolonged darkness, PhyB
1265 changes conformation again and dissociates from Pif3.

1266 The photoreceptive core of the PhyB protein contains a linear tetrapyrrole chromophore.[136] In plants,
1267 this chromophore is phytochromobilin. However, phytochromobilin is not produced in many model
1268 organisms. Thus, to use PhyB-Pif3, one adds phycocyanobilin (PCB), which is a precursor of
1269 phytochromobilin in plants and a chromophore in algal phytochromes, to the incubation medium
1270 prior to optogenetic experiments. It has been shown that bacterial and fungal phytochromes can
1271 carry biliverdin, another tetrapyrrole molecule, as a chromophore.[136]

1272

1273 # Supplementary Note 4: Tetracycline-regulated gene expression
1274 systems

1275 Tetracycline-responsive systems, originally identified in bacteria as part of a feedback loop that
1276 mediates resistance to the antibiotic tetracycline, are widely used for controlling transcription. The
1277 system is made up of the tTA regulator, which binds the *tetO* DNA sequence. In its original form, tTA is
1278 part of the Tet-Off system that is inhibited by tetracycline or the closely related molecule
1279 doxycycline[137]. Mutations that reverse tTA activity with respect to the inducer have been used to
1280 construct rtTA.[81] To function as a transcriptional activator in eukaryotes, rtTA is typically fused to the
1281 VP16 transactivation domain. To construct an inducible eukaryotic promoter, the binding sites for
1282 rtTA, *tetO*, are placed next to a minimal promoter. However, this system, called the Tet-On system,
1283 exhibits high basal activity in the absence of the inducer. To circumvent this, we fused the PEST
1284 degron to rtTA, which leads to increased degradation of rtTA.

1285

# Supplementary Figures

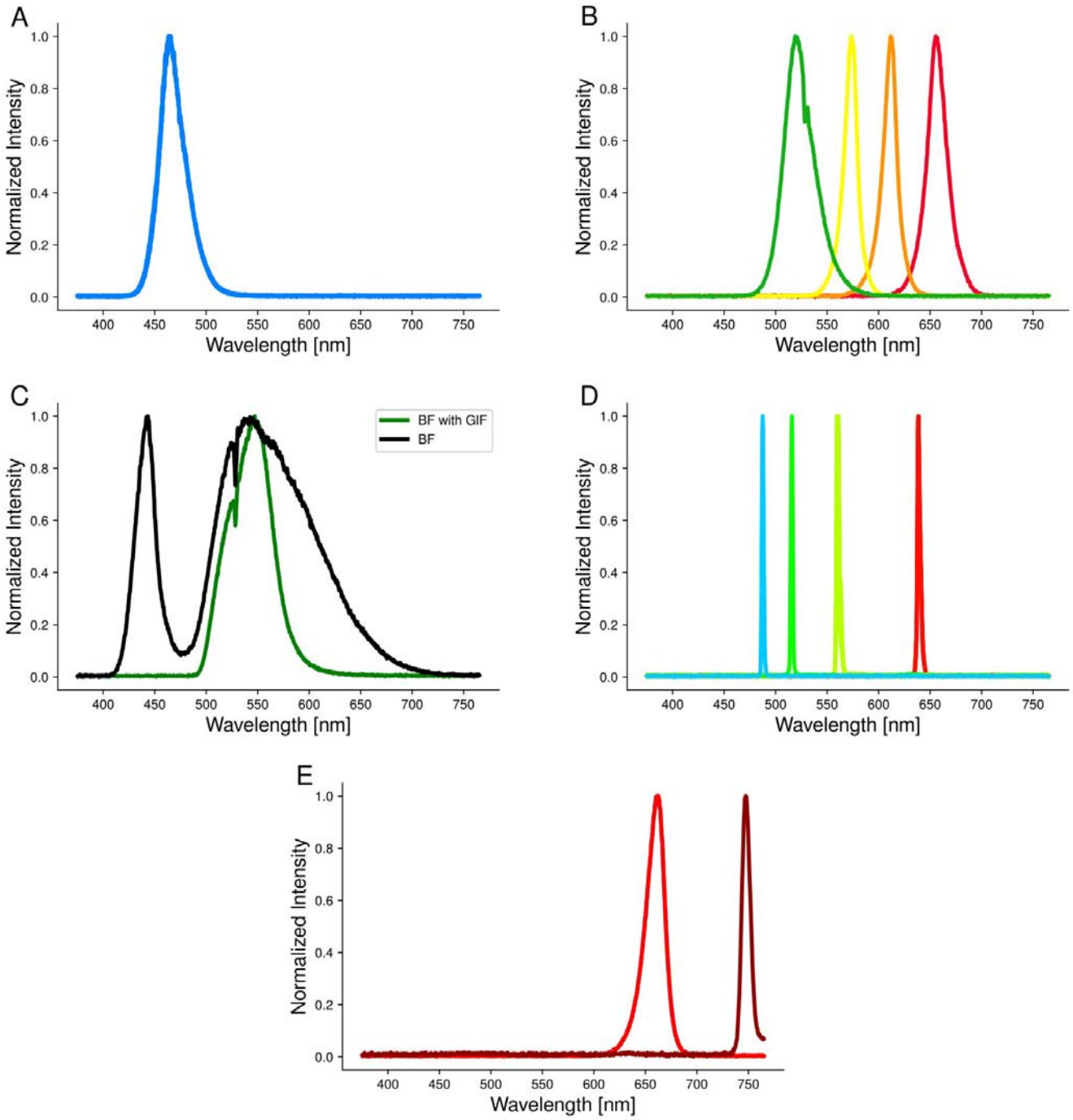


Supplementary Fig. 1. Emission spectra of light sources used. All reported intensities are total intensities and are for the location of the agar plates. A: Blue LED panel used for evolving and inducing El222 and its variants (light intensity 8.3 mW/cm$^2$). B: LEDs used to evolve color-shifted El222 variants from left to right: 24 mW/cm$^2$, 0.12 mW/cm$^2$, 2.6 mW/cm$^2$, 0.46 mW/cm$^2$. C: Diascopic LED light used for inducing El222 and its variants for microscopy. The black plot represents the spectrum of the brightfield (BF) light and the green plot is the spectrum of the same light filtered using a green interference filter (GIF). BF with GIF is used for inducing color-shifted mutants of El222 for timelapse microscopy. The

1294 intensities of the light are: 8.4 mW/cm$^2$ for BF set to 20% of the maximal power, 97 mW/cm$^2$ for BF set to 80% of maximal
1295 power, and 26 mW/cm$^2$ for BF 80% with GIF. D: Lasers used for characterizing color-shifted variants of El222. The effective
1296 light intensity of the lasers was adjusted to be the same across lasers using neutral density filters and by adjusting the
1297 duty-cycle regime of the pulsing laser light. The power intensity was 3.5 mW/cm$^2$ for all lasers. E: Red and far-red LEDs
1298 used for switching the PhyB-Pif3 system. Light intensity of the red LEDs is 36 mW/cm$^2$, and the light intensity of the far-red
1299 LEDs is 26 mW/cm$^2$.

1300

1301

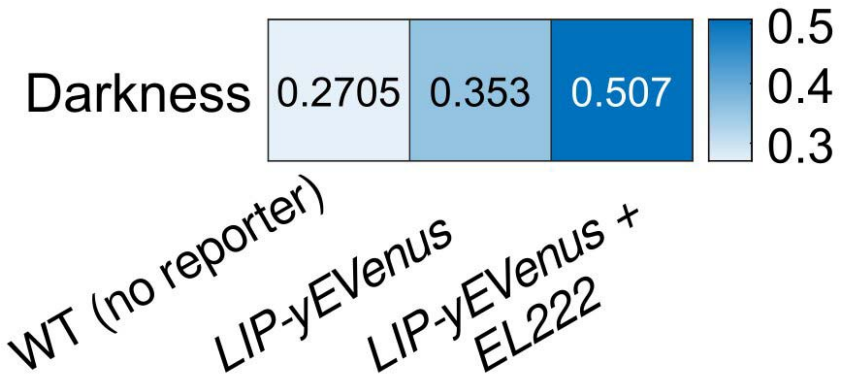


1302

1303 Supplementary Fig. 2. Baseline leakiness of the reporter sets the minimum leakiness attainable in optovolution.
1304 Comparison of fluorescence in no-reporter (WT), reporter-only (*LIP-yEVenus*), and reporter plus El222 strains (*LIP-yEVenus*
1305 *+ EL222*) in darkness. Cells that contain a transcriptional reporter for El222 (*LIP-yEVenus*) but not the transcription factor
1306 (e.g., *PGK1pr-EL222*) showed elevated fluorescence compared to wild-type budding yeast cells. This suggests that other
1307 transcription factors might weakly drive the transcription from *LIP* and set the lower bound for leakiness of *LIP*. The
1308 leakiness reported for all El222 variants is the difference between the reporter-only and the reporter plus variant strains.
1309 Numbers of analyzed cells are given in the Supplementary Table 10.

1310

1311

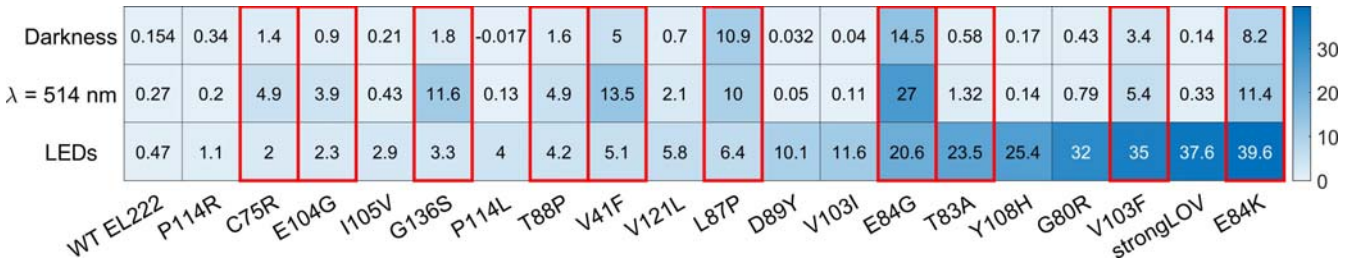


Supplementary Fig. 3. Level of activity of El222 mutants obtained in the color-shift campaign in darkness, activated by a 514 nm laser (second row), or in the presence of the green-to-red LEDs used for the campaign (third row). These measurements showed that only some of the mutants are responsive to 514 nm light. Other mutants may merely have evolved to be more sensitive to the small-wavelength tail of our green LEDs, which is why we excluded them from further analysis. We only further characterized the mutants that are substantially activated by 514 nm light. In addition, we included the L87P mutant which showed unexpected behavior by turning off in the presence of the LEDs. The values are given in percentages of 1 maxGAL1[55]. Numbers of analyzed cells are given in Supplementary Table 11.

1322 # Supplementary Tables

1323 Supplementary Table 1. Plasmids used in the study

| Plasmid name | Insert | Type of plasmid | Yeast selection marker | Bacterial selection marker | Source of the plasmid |
|---|---|---|---|---|---|
| EZL105 | *PGK1pr-EL222* | For integration in a single copy | *CgHIS3* | *AmpR* | Ref. [60] |
| pVG117 | *PGK1pr-EL222 (Asp18Tyr, Val139Leu)* | For integration in a single copy | *CgHIS3* | *AmpR* | This study |
| pVG118 | *PGK1pr-EL222 (Asp18Tyr)* | For integration in a single copy | *CgHIS3* | *AmpR* | This study |
| pVG119 | *PGK1pr-EL222 (Val139Leu)* | For integration in a single copy | *CgHIS3* | *AmpR* | This study |
| pVG135 | *PGK1pr-EL222 (Lys99Glu)* | For integration in a single copy | *CgHIS3* | *AmpR* | This study |
| pVG136 | *PGK1pr-EL222 (Pro165Ser)* | For integration in a single copy | *CgHIS3* | *AmpR* | This study |
| pVG137 | *PGK1pr-EL222 (Val201Leu)* | For integration in a single copy | *CgHIS3* | *AmpR* | This study |
| pVG120 | *PGK1pr-EL222 (Asp89Tyr)* | For integration in a single copy | *CgHIS3* | *AmpR* | This study |
| pVG147 | *PGK1pr-EL222 (Gly94Cys)* | For integration in a single copy | *CgHIS3* | *AmpR* | This study |
| pVG122 | *PGK1pr-strongLOV* | For integration in a single copy | *CgHIS3* | *AmpR* | Ref. [55] |
| pVG143 | *PGK1pr-EL222 (Leu87Ile)* | For integration in a single copy | *CgHIS3* | *AmpR* | This study |
| pVG123 | *PGK1pr-EL222 (Ala157Val)* | For integration in a single copy | *CgHIS3* | *AmpR* | This study |
| pVG286 | *PGK1pr-EL222 (Gly80Glu)* | For integration in a single copy | *CgHIS3* | *AmpR* | This study |
| pVG121 | *PGK1pr-EL222 (Gly82Val)* | For integration in a single copy | *CgHIS3* | *AmpR* | This study |
| pVG124 | *PGK1pr-EL222 (Thr83Ser)* | For integration in a single copy | *CgHIS3* | *AmpR* | This study |
| pVG310 | *PGK1pr-AQTrip* | For integration in a | *CgHIS3* | *AmpR* | This study |

| | | | | | |
|---|---|---|---|---|---|
| | (yeast codon-optimized) | single copy | | | |
| pVG150 | *PGK1pr-EL222 (Ser137Asn)* | For integration in a single copy | *CgHIS3* | *AmpR* | This study |
| pVG144 | *PGK1pr-EL222 (Val121Met)* | For integration in a single copy | *CgHIS3* | *AmpR* | This study |
| pVG178 | *PGK1pr-EL222 (Glu84Lys)* | For integration in a single copy | *CgHIS3* | *AmpR* | This study |
| pVG298 | *PGK1pr-EL222 (Thr83Ala)* | For integration in a single copy | *CgHIS3* | *AmpR* | This study |
| pVG131 | *PGK1pr-EL222 (Glu104Gly)* | For integration in a single copy | *CgHIS3* | *AmpR* | This study |
| pVG142 | *PGK1pr-EL222 (Cys75Arg)* | For integration in a single copy | *CgHIS3* | *AmpR* | This study |
| pVG132 | *PGK1pr-EL222 (Thr88Pro)* | For integration in a single copy | *CgHIS3* | *AmpR* | This study |
| pVG138 | *PGK1pr-EL222 (Gly136Ser)* | For integration in a single copy | *CgHIS3* | *AmpR* | This study |
| pVG126 | *PGK1pr-EL222 (Val103Phe)* | For integration in a single copy | *CgHIS3* | *AmpR* | This study |
| pVG139 | *PGK1pr-EL222 (Val41Phe)* | For integration in a single copy | *CgHIS3* | *AmpR* | This study |
| pVG252 | *PGK1pr-EL222 (Leu87Pro)* | For integration in a single copy | *CgHIS3* | *AmpR* | This study |
| pVG134 | *PGK1pr-EL222 (Glu84Gly)* | For integration in a single copy | *CgHIS3* | *AmpR* | This study |
| pVG101 | *PGK1pr-EL222, LIP-CLN2, LIP-CLB5* | For integration | *NatMX* | *AmpR* | This study |
| pVG104 | *ADH1pr-PHYB, ADH1pr-PIF3, GAL1-CLB5* | For integration | *NatMX* | *AmpR* | This study |
| pVG329 | *YOR1 3'UTR and YOR1 5'UTR* | For ORF replacement | *HphMX* | *AmpR* | This study |
| pVG84 | *GAL1pr-CLN2* | For integration | *PatMX* | *AmpR* | This study |
| pVG48 | *GAL1pr-yEVenus-PEST* | For integration in a single copy | *URA3* | *AmpR* | Ref. [55] |
| pVG9 | *LIP-yEVenus-PEST* | For integration in a single copy | *URA3* | *AmpR* | Ref. [55] |
| pVG175 | *LIP-ymScarletI* | For integration in a | *URA3* | *AmpR* | This study |

| | | | | | |
|---|---|---|---|---|---|
| | | single copy | | | |
| pVG176 | *LIP-ymScarletI-PEST* | For integration in a single copy | *URA3* | *AmpR* | This study |
| pVG295 | *PGK1pr-EL222, LIP-PEST-rtTA, tetOpr-CLN2* | For integration | *NatMX* | *AmpR* | This study |
| pRD-TW1 (pRD13) | *MET3pr-CLN2, CLB5pr-CLB5* | *CEN/ARS* | *URA3* | *AmpR* | This study |
| pRD70 | *tetOpr-CLB5* | For integration | *PatMX* | *AmpR* | This study |
| pVG336 | *PGK1pr-PEST-rtTA* | For integration in a single copy | *HIS3* | *AmpR* | This study |
| pVG337 | *PGK1pr-PEST-rtTA (Phe67Cys)* | For integration in a single copy | *HIS3* | *AmpR* | This study |
| pVG338 | *PGK1pr-PEST-rtTA (Arg253His)* | For integration in a single copy | *HIS3* | *AmpR* | This study |
| pVG183 | *LIP-URA3* | For integration in a single copy | *LEU2* | *AmpR* | This study |
| pVG188 | *PGK1pr-EL222, LIP-CLN2* | For integration in a single copy | *NatMX* | *AmpR* | This study |
| pVG189 | *PGK1pr-EL222, LIP-CLB5* | For integration in a single copy | *NatMX* | *AmpR* | This study |
| pVG70 | *PGK1pr-EL222, LIP-CDC20* | For integration | *NatMX* | *AmpR* | This study |
| pVG15k | *PGK1pr-EL222, LIP-CLB2kd* | For integration | *NatMX* | *AmpR* | This study |
| pVG47 | *tetOpr-yEVenus-PEST* | For integration in a single copy | *URA3* | *AmpR* | Ref. [55] |

1324

1325

1326 Supplementary Table 2. Strains used in the study

| Strain name | Genotype | Source |
|---|---|---|
| yVG602 | *cln1,3Δ cln2Δ::MET3pr-CLN2 clb1Δ clb2Δ::GALL-CLB2::URA3 HTB2::HTB2-mCherry::HIS3 PGK1pr::PGK1pr-EL222, LIP-CLB2::NatMX* | This study |
| yVG173 | *clb1Δ clb2Δ::GALL-CLB2::URA3 clb3Δ::TRP1 clb4Δ::his3::kanMX clb5Δ::kanMX clb6Δ::kanMX swe1Δ::TRP1 PGK1pr::PGK1pr-EL222, LIP-CLB2kd::NatMX ADE2* | This study |
| yVG604 | *cdh1Δ::LEU2 cdc20Δ::MET3pr-CDC20::TRP1 CLN2pr-GFP-CLN2pest::HIS3 PGK1pr::PGK1pr-EL222, LIP-CDC20::NatMX* | This study |
| yVG152 | *cln1Δ cln2Δ::CLN2pr-Venus::TRP1 cln3Δ::LEU2 trp1Δ::MET3-CLN2::TRP1 clb3Δ::TRP1 clb4Δ::his3::KanMX clb6Δ::KanMX HTB2::HTB2-mCherry::HIS5 PGK1pr::PGK1pr-EL222, LIP-CLB5::NatMX* | This study |
| yVG2371 | *cln1Δ cln2Δ cln3Δ::LEU2 trp1Δ::MET3pr::CLN2 ycr051wΔ::PGL1pr-EL222, LIP-CLN2::NatMX* | This study |
| yVG2374 | *cln1Δ cln2Δ cln3Δ::LEU2 trp1Δ::MET3pr::CLN2 ycr051wΔ::PGL1pr-EL222, LIP-CLB5::NatMX* | This study |
| yVG2390 | *cln1Δ cln2Δ cln3Δ::LEU2 clb3Δ::TRP1 clb4Δ::his3::KanMX clb5Δ::HIS3 clb6Δ::KanMX HTB2::HTB2-mCherry::HIS5 POL3::POL3 (Leu523Asp)::hphMX EFB1pr::PGK1pr-EL222, LIP-CLB5::NatMX pRD-TW1 (CEN/ARS)* | This study |
| yVG1247 | *cln1Δ cln2Δ cln3Δ::LEU2 clb3Δ::TRP1 clb4Δ::his3::KanMX clb5Δ::HIS3 clb6Δ::KanMX HTB2::HTB2-mCherry::HIS5 POL3::POL3 (Leu523Asp)::hphMX EFB1pr::PGK1pr-EL222, LIP-CLN2, LIP-CLB5::NatMX* (single copy) | This study |
| yVG1358 | *cln1Δ cln2Δ cln3Δ::LEU2 clb3Δ::TRP1 clb4Δ::his3Δ::KanMX clb5Δ::HIS3 clb6Δ::KanMX HTB2::HTB2-mCherry::HIS5 POL3::POL3 (Leu523Asp)::hphMX sic1Δ::URA3 EFB1pr::PGK1pr-EL222, LIP-CLN2, LIP-CLB5::NatMX* (single copy) | This study |

| | | |
|---|---|---|
| yVG1623 | *ura3Δ::LIP-yEVenus::KanMX* (single copy) | Ref. [55] |
| yVG2840 | *ycr051wΔ::LIP-ymScarletI::URA3* (single copy) | This study |
| yVG2842 | *his3Δ::PGK1pr-EL222::HIS3* (single copy) *ycr051wΔ::LIP-ymScarletI-PEST::URA3* (single copy) | This study |
| yVG1637 | *his3Δ::PGK1pr-EL222::HIS3* (single copy) *ura3Δ::LIP-yEVenus::KanMX* (single copy) | Ref. [55] |
| yVG2844 | *his3Δ::PGK1pr-EL222 (Asp18Tyr, Val139Leu)::HIS3* (single copy) *ura3Δ::LIP-yEVenus::KanMX* (single copy) | This study |
| yVG2846 | *his3Δ::PGK1pr-EL222 (Asp18Tyr)::HIS3* (single copy) *ura3Δ::LIP-yEVenus::KanMX* (single copy) | This study |
| yVG2848 | *his3Δ::PGK1pr-EL222 (Val139Leu)::HIS3* (single copy) *ura3Δ::LIP-yEVenus::KanMX* (single copy) | This study |
| yVG2850 | *his3Δ::PGK1pr-EL222 (Lys99Glu)::HIS3* (single copy) *ura3Δ::LIP-yEVenus::KanMX* (single copy) | This study |
| yVG2852 | *his3Δ::PGK1pr-EL222 (Pro165Ser)::HIS3* (single copy) *ura3Δ::LIP-yEVenus::KanMX* (single copy) | This study |
| yVG2854 | *his3Δ::PGK1pr-EL222 (Val201Leu)::HIS3* (single copy) *ura3Δ::LIP-yEVenus::KanMX* (single copy) | This study |
| yVG2701 | *his3Δ::PGK1pr-EL222 (Asp89Tyr)::HIS3* (single copy) *ycr051wΔ::LIP-ymScarletI::URA3* (single copy) | This study |
| yVG2750 | *his3Δ::PGK1pr-EL222 (Gly94Cys)::HIS3* (single copy) *ycr051wΔ::LIP-ymScarletI::URA3* (single copy) | This study |
| yVG2704 | *his3Δ::PGK1pr-strongLOV::HIS3* (single copy) *ycr051wΔ::LIP-ymScarletI::URA3* (single copy) | This study |
| yVG2726 | *his3Δ::PGK1pr-EL222 (Leu87Ile)::HIS3* (single copy) *ycr051wΔ::LIP-ymScarletI::URA3* (single copy) | This study |
| yVG1645 | *his3Δ::PGK1pr-EL222 (Ala157Val)::HIS3* (single copy) *ura3Δ::LIP-yEVenus::KanMX* (single copy) | This study |
| yVG2759 | *his3Δ::PGK1pr-EL222 (Gly80Glu)::HIS3* (single copy) *ycr051wΔ::LIP-ymScarletI::URA3* (single copy) | This study |
| yVG2703 | *his3Δ::PGK1pr-EL222 (Gly82Val)::HIS3* (single copy) | This study |

| | | |
|---|---|---|
| | *ycr051wΔ::LIP-ymScarletI::URA3* (single copy) | |
| yVG2706 | *his3Δ::PGK1pr-EL222 (Thr83Ser)::HIS3* (single copy) *ycr051wΔ::LIP-ymScarletI::URA3* (single copy) | This study |
| yVG2761 | *his3Δ::PGK1pr-AQTrip (yeast codon optimized)::HIS3* (single copy) *ycr051wΔ::LIP-ymScarletI::URA3* (single copy) | This study |
| yVG2752 | *his3Δ::PGK1pr-EL222 (Ser137Asn)::HIS3* (single copy) *ycr051wΔ::LIP-ymScarletI::URA3* (single copy) | This study |
| yVG2727 | *his3Δ::PGK1pr-EL222 (Val121Met)::HIS3* (single copy) *ycr051wΔ::LIP-ymScarletI::URA3* (single copy) | This study |
| yVG2753 | *his3Δ::PGK1pr-EL222 (Glu84Lys)::HIS3* (single copy) *ycr051wΔ::LIP-ymScarletI::URA3* (single copy) | This study |
| yVG2699 | *his3Δ::PGK1pr-EL222 (Thr83Ala)::HIS3* (single copy) *ycr051wΔ::LIP-ymScarletI::URA3* (single copy) | This study |
| yVG2714 | *his3Δ::PGK1pr-EL222 (Glu104Gly)::HIS3* (single copy) *ycr051wΔ::LIP-ymScarletI::URA3* (single copy) | This study |
| yVG2725 | *his3Δ::PGK1pr-EL222 (Cys75Arg)::HIS3 (single copy)* *ycr051wΔ::LIP-ymScarletI::URA3* (single copy) | This study |
| yVG2715 | *his3Δ::PGK1pr-EL222 (Thr88Pro)::HIS3* (single copy) *ycr051wΔ::LIP-ymScarletI::URA3* (single copy) | This study |
| yVG2721 | *his3Δ::PGK1pr-EL222 (Gly136Ser)::HIS3 (single copy)* *ycr051wΔ::LIP-ymScarletI::URA3* (single copy) | This study |
| yVG2709 | *his3Δ::PGK1pr-EL222 (Val103Phe)::HIS3* (single copy) *ycr051wΔ::LIP-ymScarletI::URA3* (single copy) | This study |
| yVG1031 | *ura3Δ::GAL1pr-yEVenus::KanMX* | Ref. [55] |
| yVG301 | *ura3Δ::GAL1pr-yEVenus-PEST::URA3* | Ref. [55] |
| yVG151 | *PHYB-mCherry-Tom7::LEU2; Bem1-mCitrine-PIF::HIS3* | Ref. [107] |
| yVG2839 | *PHYB-mCherry-Tom7::LEU2; Bem1-mCitrine-PIF::HIS3 yor1::hphMX* | This study |

| | | |
|---|---|---|
| yVG2837 | *leu2Δ::ADH1pr-GADPIF3::LEU2, trp1::ADH1pr-PHYB-GDBD::TRP1, his3Δ::GAL1pr-YFP::HIS3, ade2::ADE2* | Ref. [76] |
| yVG2838 | *leu2Δ::ADH1pr-GADPIF3::LEU2, trp1::ADH1pr-PHYB-GDBD::TRP1, his3Δ::GAL1pr-YFP::HIS3, ade2::ADE2 yor1::hphMX* | This study |
| yVG2265 | *his3Δ::PGK1pr-EL222::HIS3* (single copy) *ycr051wΔ::LIP-URA3::LEU2* (single copy) | This study |
| yVG2691 | *cln1Δ cln2Δ cln3Δ::LEU2 clb3::TRP1 clb4Δ::his3Δ::KanMX clb5Δ::HIS3 clb6Δ::KanMX HTB2::HTB2-mCherry::HIS5 ycr051wΔ::PGK1pr-EL222, LIP-PEST-rtTA, tetOpr-CLN2::NatMX BUD23::tetOpr-CLB5::PatMX* | This study |
| yVG2856 | *his3Δ::PGK1pr-PEST-rtTA::HIS3* (single copy) *ura3Δ::tetOpr-yEVenus-PEST::URA3* (single copy) | This study |
| yVG2857 | *his3Δ::PGK1pr-PEST-rtTA (Phe67Cys)::HIS3* (single copy) *ura3Δ::tetOpr-yEVenus-PEST::URA3* (single copy) | This study |
| yVG2858 | *his3Δ::PGK1pr-PEST-rtTA (Arg253Hys)::HIS3* (single copy) *ura3Δ::tetOpr-yEVenus-PEST::URA3* (single copy) | This study |

1329 Supplementary Table 3. Number of cells analyzed in Figure 2 B

| Experiment | Number of scored cells |
|---|---|
| *LIP-CLB5 cln1-3Δ 20 min pulse* | 53 |
| *LIP-CLB5 cln1-3Δ 40 min pulse* | 30 |
| *LIP-CLN2 cln1-3Δ 20 min pulse* | 27 |
| *LIP-CLN2 cln1-3Δ 40 min pulse* | 20 |
| *LIP-CLB5 cln1-3Δ clb3-6Δ pRD-TW1 20 min* | 129 |
| *LIP-CLB5 LIP-CLN2 cln1-3Δ clb3-6Δ pRD-TW1 40 min* | 42 |

1330

1331

1332 Supplementary Table 4. Number of cells analyzed in Figure 4 B

| | WT EL222 | G94C | V121M | A157V | S137N | G80E | D89Y | AQTrip | T83S | E84K | strongLOV | G82V | L87I |
|---|---|---|---|---|---|---|---|---|---|---|---|---|---|
| Darkness | 246 | 234 | 424 | 144 | 206 | 341 | 341 | 275 | 126 | 227 | 478 | 239 | 248 |
| Low blue LED | 329 | 48 | 344 | 155 | 76 | 117 | 151 | 58 | 107 | 81 | 84 | 93 | 93 |
| High blue LED | 374 | 60 | 320 | 283 | 67 | 58 | 88 | 83 | 95 | 274 | 100 | 43 | 57 |

1333

1334

1335

1336 Supplementary Table 5. Number of cells analyzed in Figure 4 C, G, and K

| Figure. | mutant | N at 3.5 h |
|---|---|---|
| 4 C | *wt-EL222* | 267 |
| 4 C | T83S | 105 |
| 4 C | G82V | 77 |
| 4 C | L87I | 119 |
| 4 C | G80R | 79 |
| 4 C | A157V | 92 |
| 4 G | *wt-EL222* | 93 |
| 4 G | K99E | 68 |
| 4 G | V201L | 31 |
| 4 K | *wt-EL222* | 121 |
| 4 K | T83A | 40 |

1337

1338

1339 Supplementary Table 6. Number of cells analyzed in Figure 4 F

| | V201L | D31Y, V139L | K99E | P165S | D31Y | V139L | WT EL222 |
|---|---|---|---|---|---|---|---|
| Darkness | 112 | 479 | 188 | 238 | 208 | 362 | 246 |
| Low blue LED | 325 | 203 | 330 | 81 | 419 | 209 | 329 |
| High blue LED | 209 | 382 | 321 | 98 | 466 | 441 | 374 |

1340

1341

1342

1343 Supplementary Table 7. Number of cells analyzed in Figure 4 J

| | WT EL222 | E104G | T83A | C75R | V103F | T88P | G136S | E84K | L87P | V41F | E84G |
|---|---|---|---|---|---|---|---|---|---|---|---|
| Darkness | 246 | 142 | 65 | 135 | 262 | 80 | 141 | 227 | 386 | 149 | 175 |
| High blue LED | 374 | 107 | 539 | 158 | 558 | 486 | 70 | 274 | 328 | 220 | 96 |
| $\lambda$ = 488 nm | 438 | 119 | 219 | 326 | 160 | 241 | 303 | 615 | 270 | 193 | 685 |
| $\lambda$ = 514 nm | 244 | 166 | 256 | 313 | 230 | 261 | 187 | 264 | 420 | 126 | 180 |
| $\lambda$ = 561 nm | 177 | 267 | 175 | 141 | 204 | 182 | 188 | 204 | 197 | 156 | 101 |
| $\lambda$ = 651 nm | 202 | 237 | 113 | 232 | 191 | 189 | 183 | 269 | 275 | 278 | 206 |

1344

1345

1346

1347 Supplementary Table 8. Number of cells analyzed in Figure 6 C

| | Darkness, no PCB | Darkness, PCB | Light, no PCB | Light, PCB |
|---|---|---|---|---|
| *yor1Δ* | 133 | 75 | 143 | 71 |
| *YOR1* | 186 | 83 | 181 | 190 |

1348

1349

1350

1351 Supplementary Table 9. Number of cells analyzed in Figure 7 D

| | WT | F67C | R253H |
|---|---|---|---|
| + Dox | 220 | 506 | 467 |
| - Dox | 178 | 273 | 321 |

1352

1353

1354

1355 Supplementary Table 10. Number of cells analyzed in Supplementary Figure 2.

| | AX42 | LIP-yEVenus | WT EL222 |
|---|---|---|---|
| Darkness | 229 | 433 | 246 |

1356

1357

1358

1359 Supplementary Table 11. Number of cells analyzed in Supplementary Figure 3.

| | D89Y | V103I | P114L | Y108H | P114R | WT EL222 | strongLOV | I105V | G80R | T83A | V121L | E104G | T88P | C75R | V103F | L87P | E84K | G136S | V41F | E84G |
|---|---|---|---|---|---|---|---|---|---|---|---|---|---|---|---|---|---|---|---|---|
| Darkness | 341 | 183 | 110 | 133 | 217 | 246 | 478 | 114 | 240 | 65 | 198 | 142 | 80 | 135 | 262 | 386 | 227 | 141 | 149 | 175 |
| 514 nm | 198 | 331 | 230 | 272 | 324 | 244 | 502 | 105 | 365 | 256 | 127 | 166 | 261 | 313 | 230 | 420 | 264 | 187 | 126 | 180 |

1360

1361